Paper IV

Mechanistic study of asymmetric Co-catalyzed hydrogenation of enamides

Ljiljana Pavlovic, Hongyu Zhong, Paul J. Chirik and Kathrin H. Hopmann
(*In preparation*)

Manuscript Draft

Mechanistic study of asymmetric Co-catalyzed hydrogenation of enamides

Ljiljana Pavlovic,[a] Hongyu Zhong,[b] Paul J. Chirik,[b] Kathrin H. Hopmann[a]

[a]Hylleraas Centre for Quantum Molecular Sciences, Department of Chemistry, UiT The Arctic University of Norway, N-9037 Tromsø, Norway
[b]Department of Chemistry, Princeton University, New Jersey 08544, United States.

ABSTRACT: We investigated the asymmetric cobalt-diphosphine-catalyzed hydrogenation of enamides using density functional theory. The reactivity of two enamides with significantly different molecular structure was evaluated: *dehydro*-levetiracetam and methyl 2-acetamidoacrylate. Our results indicate that both substrates prefer a non-redox Co(II) mechanism, featuring four and five-membered metallacycle intermediates for *dehydro*-levetiracetam and 6-membered metallacycles for methyl 2-acetamidoacrylate. However, for each substrate, a redox Co(0)/Co(II) mechanism appears to be only slightly higher in energy, indicating that for the Co-^{Ph}BPE-catalyzed hydrogenation of enamides, both redox and non-redox pathways compete under reaction conditions. Explicit solvent is found to be crucial for stabilization of transition states and for the proper estimation of the enantiomeric excess of Co-^{Ph}BPE-catalyzed hydrogenation.

INTRODUCTION

In homogeneous hydrogenation catalysis, increasing attention is devoted towards the use of earth-abundant 3*d* metals instead of their precious counterparts.[1,2] The motivation to use non-noble metals lies in their abundance, lower toxicity and reasonable cost.[3] However, the 3*d* transition metals may have different properties than precious metal systems. Whereas the latter typically react via two electron processes, including elementary steps such oxidative addition and reductive elimination,[4-7] 3*d* metals have more accessible oxidation states, allowing for additional one-electron processes.[8] They may also simultaneously display redox and non-redox pathways,[9] making the search for their reaction mechanisms more unpredictable and challenging.

In a recent perspective, Arevalo and Chirik have given an overview of strategies that can be used to enable two electron redox chemistry with first row transition metals.[10] However, although many experimental[11-22] and computational hydrogenation studies[9,23-28] have been reported with 3*d* transition metal catalysts, the use of such systems in enantioselective hydrogenation remains less explored.[29-38] Examples include Fe-based asymmetric hydrogenation of ketones[35,38] and imines,[37] and Co-based protocols for asymmetric hydrogenation of alkenes.[2,29,30,33,39]

Recently, Chirik and co-workers reported the Co-catalyzed asymmetric hydrogenation of enamides[33] and showed that chiral bidentate phosphine ligands, known to give good enantioselectivities in Rh and Ru-based hydrogenations,[40,41] also provide excellent results with cobalt. The optimal reaction conditions were found with $CoCl_2$ and Zn dust as an activator, in MeOH at 50 °C. More than two hundred chiral ligands were tested, and among others, (*R*,*R*)-^{Ph}BPE and (*R*,*R*)-^{iPr}DuPhos displayed high activity and enantioselectivity with enamides (Table 1).

We have previously shown that achiral cobalt-diphosphine complexes may access different mechanisms for hydrogenation of hydroxylated and non-hydroxylated alkenes.[9] Whereas non-hydroxylated alkenes appear to be hydrogenated through a redox pathway cycling between Co(0) and Co(II) states, hydroxylated alkenes prefer a non-redox Co(II) metallacyle pathway. The hydroxyl group in the studied substrates was placed minimum one atom from the double bond, with the computational results indicating that its primary function was to form a stable metallacycle intermediate.[9] It is unclear at this stage which mechanism is preferred in the Co-mediated hydrogenation of enamides, which have a functional group (NR) *directly* at the double bond. We envision that several putative mechanistic alternatives arise for cobalt-catalyzed enamide hydrogenation, in particular in presence of substituents that have the potential to be deprotonated (e.g NH_2, Scheme 1, **A-D**). The possible Co(0)-Co(II) redox mechanism **A** has been proposed for different Co-diphosphine systems.[9,22,29,33,42]

Table 1. Selected examples of (*R*,*R*)-^{Ph}BPE-Co-mediated enamide hydrogenation.[33]

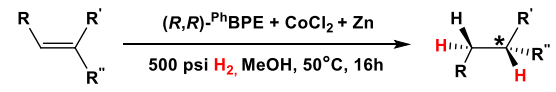

Substrate	Product	% Yield	% e.e.
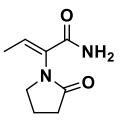	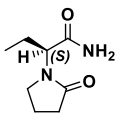	99.8 (0.20% [Co])	98.3
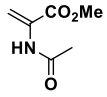	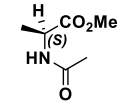	100 (10 mol% [Co])	85.0

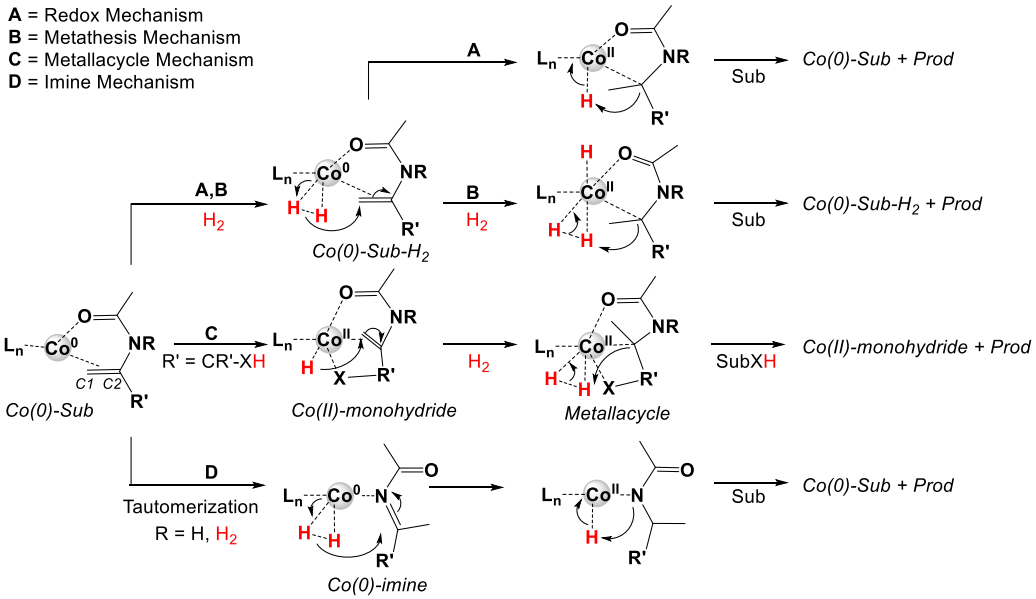

Scheme 1. Possible mechanisms for the Co-catalyzed hydrogenation of enamides (for discussion and references, see main text). Mechanism **A**, **B**, **C** are shown with initial hydride transfer to C1, but C2 is also possible. For **D**, initial transfer to N is also possible.

Mechanism **B** is a σ-bond metathesis pathway related to proposals for alkene hydrogenation with Co(I)-diminopyridine complexes.[24,32] Mechanism **C** was proposed by us for the cobalt-diphosphine-catalyzed hydrogenation of hydroxylated alkenes.[9] Due to the possibility that enamides may tautomerize to imines, additional mechanistic possibilities arise. Mechanism **D** is related to the mechanisms studied for Ir-catalyzed imine hydrogenation[43,44] and was also recently considered in Co-mediated imine reduction.[45]

In this study, we have computationally evaluated the Co-(*R*,*R*)-^{Ph}BPE-catalyzed hydrogenation of two enamides with distinct molecular structures to establish their preferred mechanistic routes and to obtain insights into the factors controlling their enantioselective conversion.

METHODS

Computational models: Full molecular systems, consisting of the Co-(*R*,*R*)-^{Ph}BPE catalyst and the substrates, was computed (Fig. 1), without truncations or symmetry constrains. A low-spin S = ½ spin state was employed in the computations, as determined experimentally for the (*R*,*R*)-^{Ph}BPE-Co complex.[33] Computational evaluation of the quartet state confirmed that it is higher in energy. Zn was not included in the model, as the experimental studies have shown that it is not needed if the hydrogenation sets out from the Co(0) species.[33]

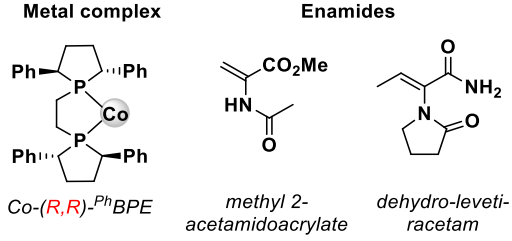

Figure 1. Metal complex and substrates studied here.

Computational methods: All geometry optimization and frequency calculations were performed with the Gaussian09 package, Rev. D01.[46] The DFT hybrid functional B3LYP was employed with the Grimme empirical dispersion correction.[47] The IEFPCM model was used in order to include solvent effect (methanol solvent).[48,49] For the geometry optimizations, the small 6-311G (d,p) (BS1) basis set was used on all non-metals, whereas the basis set and the pseudopotential LANL2TZ was used on Co. The optimized structures displayed only real vibrational frequencies, with the exception of all transition states structures, which exhibited one imaginary frequency. In order to obtain more accurate energies, single point calculations were performed with 6-311++G(2df,2pd) on all non-metals, whereas the basis set and the pseudopotential LANL2TZ was used on Co (BS2). Counter poise corrections computed at the BS2 level (CP_{BS2}) were included in order to correct for the artificial lowering of the electronic energy, caused by the borrowing of basis functions when molecular fragments are joined into one model. The computed free energies (ΔG°1atm, BS1) in the gas phase were converted into the corresponding 1M standard state energies, employing a standard state (SS) conversion term.[50] Only reactions where the number of moles are changed are affected. For the reaction A + B = C at 323.15 K, SS = -2.1 kcal/mol. For reactions involving explicit solvent, the standard state of the solvent is employed, which is 4.2 kcal/mol (based on the concentration of the pure solvent of 24.7 M for MeOH, derived from the density of 0.792 g/mL). Temperature corrections were included in all free energies to match the experimental temperature (50 °C). The standard state Gibbs free energies ($\Delta G°_{1M,323K}$) reported in the main text corresponds to:

(eq.1) $\Delta G°_{1M,323K} = \Delta G_{1atm,\,323K,BS1} - \Delta E_{1atm,BS1} + \Delta E_{1atm,BS2} + CP_{BS2} + SS_{323K}$

Enantioselectivities were evaluated from the computed barriers for the rate limiting steps using the following fomula:[51]

(eq. 2) $$ee_{theo} = \frac{1-e^{\left(-\frac{\Delta\Delta G^{\#}}{RT}\right)}}{1+e^{\left(-\frac{\Delta\Delta G^{\#}}{RT}\right)}} * 100$$

Experimental details: [to be filled by collaborators]

RESULTS AND DISCUSSION

Several possible mechanistic pathways for Co-(*R*,*R*)-^{Ph}BPE-catalyzed hydrogenation of enamides (Scheme 1) were studied using DFT methods on the full molecular systems (Figure 1). Detailed schematic drawings and energies for all pathways are found in the Supporting Information (SI).

Hydrogenation of *dehydro*-levetiracetam: The Co-mediated hydrogenation of *dehydro*-levetiracetam (Table 1) leads to the chiral epilepsy drug Keppra.[33] This substrate is interesting, because in addition to the enamide functional group, it possesses an ionizable primary amide, making mechanisms **A** to **C** possible options (Scheme 1). Tautomerization of *dehydro*-levetiracetam to a neutral imine is not possible, excluding mechanism D.

Hydrogenation of *dehydro*-levetiracetam via a redox-type mechanism **A** sets out from a substrate-coordinated species, where the enamide coordinates to cobalt through both the double bond and the oxygen atom of the amide motif (Fig. 2). A similar coordination mode has been observed in the X-ray structure of the enamide methyl 2-acetamidoacrylate with a cationic Co-DuPhos complex,[2] however, the orientation of *dehydro*-levetiracetam is different.[52]

Our computations show a very high dissociation energy of almost 50 kcal/mol for the substrate (SI, Fig. S1), indicating that the enamide-coordinated complex is rather stable. It is thus unlikely that cobalt will be uncoordinated when H_2 binds, as has been assumed in other studies on Co-catalyzed alkene or imine hydrogenation via a redox mechanism.[2,42] Coordination of H_2 to the substrate-coordinated complex leads to formation of a Co(0)-H_2-Sub species, where H_2 prefers to form a σ-bonded complex and is not oxidatively added to Co. In the next step of Mechanism **A**, an oxidative hydride transfer to the C2 atom (TS_Hyd) gives an alkyl intermediate, which has a computed barrier of 26.5 kcal/mol with the *pro*-(*S*) coordinated substrate (SI, Fig. S2). TS_Hyd is the rate- and selectivity-determining step of mechanism **A**. At the intermediate, the substrate behaves as a chelate and interacts with cobalt through both the nucleophilic carbon and the amide oxygen. Finally, reductive elimination liberates the product and regenerates the Co(0) species (SI, Fig. S2). An overall barrier of 26.5 kcal/mol would be feasible at the experimental temperature of 323 K (based on the discussion by Baik and coworkers, a reasonable conversion at 323K requires a barrier below 27.1 kcal/mol).[53]

Mechanism **B** starts similar as Mechanism **A** with a hydride transfer to the substrate (SI, Fig. S3). Then an additional H_2 molecule binds, which transfers a proton to the substrate. This σ-bond methathesis pathway has a computed barrier of 37.7 kcal/mol, making it non-feasible.

The non-redox metallacycle mechanism **C** starts from a Co(II)-monohydride species (Scheme 2), which is 10.0 kcal/mol above the reference structure Co(0)-Sub. Hydride transfer to the C2 atom of the enamide has a barrier of only 18.0 kcal/mol and forms an interesting four-membered metallacycle intermediate (Fig. 2). The conformer formed right after hydride transfer does not have the substrate carbonyl coordinated to Co (Co-metallacycle, conformer 1, Fig. 2), however, upon recoordination of the carbonyl, the metallacycle intermediate exhibits a low relative energy of -3.5 kcal/mol (Co-metallacycle, conformer 2, Fig. 2). In the next step, H_2 coordination takes place, followed by proton transfer to the C3 atom to form the hydrogenated Co(II)-Int-H intermediate, with a barrier of 23.7 kcal/mol. This step is thus rate- and selectivity-determining.[54] In the final step, coordination of another substrate occurs, which transfers its proton to the nitrogen atom (barrier of 15.7 kcal/mol relative to the lowest-lying intermediate), resulting in the final product and the regeneration of the active Co(II)-monohydride species.

We also tested another variant of the metallacycle mechanism **C** (SI, Figure S4), where the initial hydride transfer occurs to the C3 atom of the substrate. The formed intermediate is now a five-membered metallacycle species. The following steps are the same as for the four-membered metallacycle, with the only difference that subsequent proton transfer occurs to the C2 atom.

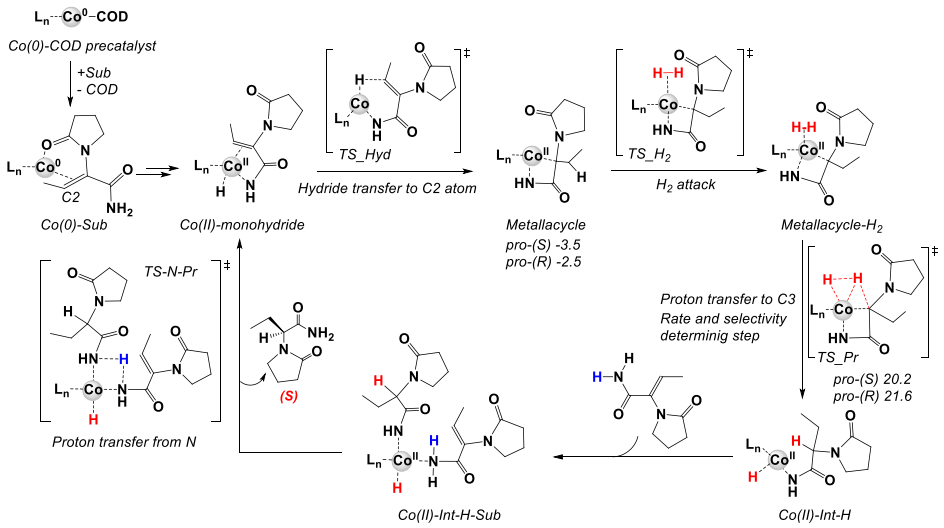

Scheme 2. Non-redox metallacycle mechanism **C** for the Co-^{Ph}BPE-catalyzed hydrogenation of *dehydro*-levetiracetam. Free energies of the 4-membered metallacycle intermediates and rate-limiting proton transfer TSs are given in kcal/mol, 323 K, relative to Co(0)-Sub.

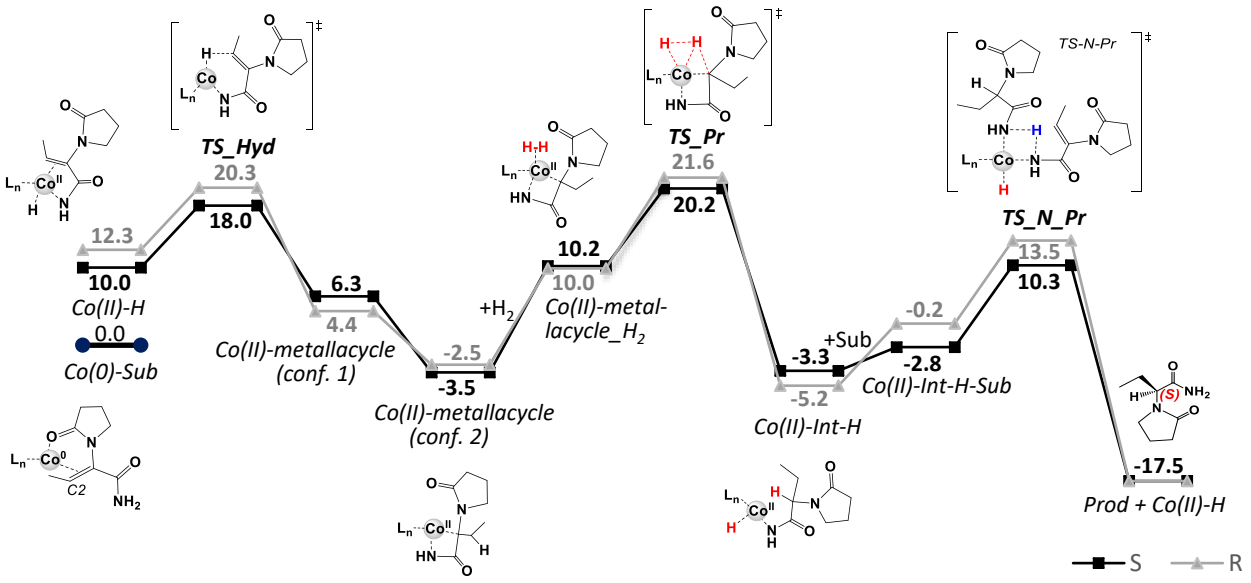

Figure 2. Computed energy profiles profile (kcal/mol, 323 K, B3LYP-D3/BS2[IEFPCM]//B3LYP-D3//BS1[IEFPCM] level of theory) for the Co-^{Ph}BPE-catalyzed hydrogenation of *dehydro*-levetiracetam via metallacycle mechanism **C**, including (*R*) and (*S*) pathways Energies are given relative to Co(0)-Sub.

Interestingly, the rate-determining step for the formation of the predominant (*S*)-product is the hydride transfer step with a barrier of 23.8 kcal/mol, yet the rate-limiting step for the formation of the (*R*)-product is the proton transfer step with a barrier of 24.0 kcal/mol.

The computed energies indicate that for Co-^{Ph}BPE-catalyzed hydrogenation of *dehydro*-levetiracetam, both four-membered and five-membered metallacycle mechanisms are energetically feasible at the reaction temperature of 323 K. However, a relevant question is how the active monohydride species initially is formed in Mechanism **C**. In the Co(II)-dialkyl-mediated hydrogenation of hydroxylated alkenes, we proposed that a Co(II)-monohydride species can be formed from the Co(II) precatalyst through protonation and loss of the alkyl ligands.[9] However, for the current system, the starting complex is a Co(0) species with a neutral ligand,[33] making it less obvious how a Co(II)-monohydride can be formed. A direct oxidative addition of the ionizable group of the substrate to Co(0) is too costly with a barrier of 42.2 kcal/mol (SI, Fig. S5). Instead, we propose that the reaction starts from the Co(0)-enamide species, which binds H_2 and undergoes a hydride transfer to the enamide (Scheme 3). The formed hydride may then abstract a proton from the ionizable group of the substrate (here XH = NH_2), resulting in formation of the metallacycle that is part of Mechanism **C**. The barrier from Co(0)-Sub to the metallacycle is 26.5 kcal/mol, making it feasible to occur once at the reaction temperature. After the metallacycle is formed, mechanism **C** can operate in subsequent reaction cycles (overall barrier 23.7 kcal/mol).

In conclusion, it appears that the metallcycle mechanism **C** is preferred for Co-^{Ph}BPE-catalyzed hydrogenation of *dehydro*-levetiracetam (barriers of 23.7 to 24.0 kcal/mol for the (*S*) and (*R*) pathways, Scheme 2 and Fig. S4), however, it needs to be emphasized that of the other tested mechanisms, in particular mechanism **A** appears to be within reach for formation of the (*S*)-product (barrier of 26.5 kcal/mol, Figure S2).

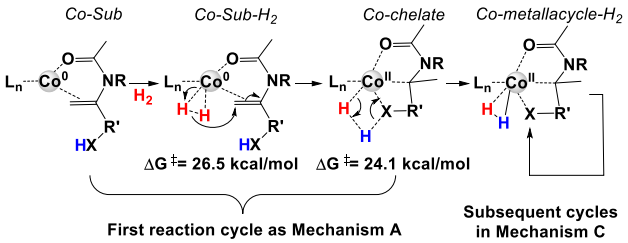

Scheme 3. Proposed route for the initial transformation of the stable Co(0)-Sub species to an intermediate in Mechanism **C**. Numbers obtained with *dehydro*-levetiracetam.

Hydrogenation of methyl 2-acetamidoacrylate: Initially we evaluated the hydrogenation of methyl 2-acetamidoacrylate via redox mechanism **A** (Figure 3). The steps are the same as discussed for *dehydro*-levetiracetam, with hydride transfer to C1 and an overall barrier of 24.3 kcal/mol for formation of the (*S*)-product, which is feasible at the experimental temperature of 323 K. If hydride transfer occurs to C2 of the enamide instead, the barrier raises to 38.7 kcal/mol (SI, Fig. S6), excluding this pathway. The alternative Mechanism **B** has a barrier of 28.6 kcal/mol (SI, Figure S7) and thus not feasible at reaction temperature. Interestingly, mechanism **C**, which proceeds via a 6-membered metallacycle, has a similar barrier as the redox mechanism **A** of 24.0 kcal/mol (SI, Fig. S8). The redox imine mechanism **D** has a minimum barrier of 28.3 kcal/mol (SI, Fig. S9). An alternative imine hydrogenation mechanism proceeding via heterolytic H_2 cleavage is not accessible (SI, Fig. S10). Thus, of all tested mechanisms, redox mechanism **A** and non-redox metallcycle mechanism **C** appear most feasible for the hydrogenation of the enamide methyl 2-acetamidacrylate. However, the inclusion of explicit solvent in the calculations has a significant impact on the computed barriers, as discussed further below.

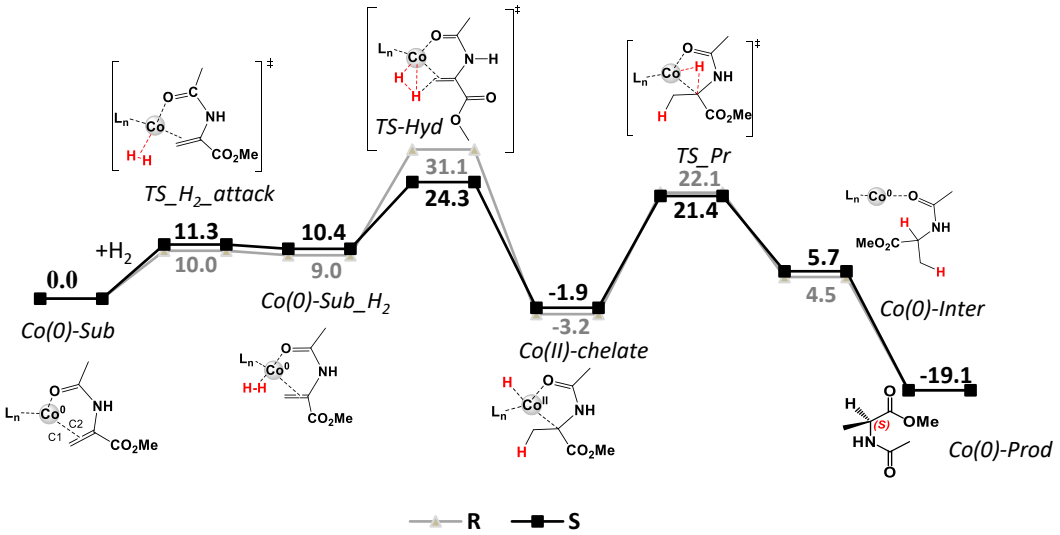

Figure 3. Computed energy profile (kcal/mol, 323 K, B3LYP-D3/BS2[IEFPCM]//B3LYP-D3//BS1[IEFPCM]) for the Co-^{Ph}BPE-catalyzed hydrogenation of methyl 2-acetamidoacrylate via redox mechanism **A**.

Effect of explicit solvent: Hydrogenation of methyl 2-acetamidoacrylate appears to be possible via both mechanism **A** and **C** (*vide supra*), however, for both pathways, the computed barriers for formation of the (*R*)-product are high, respectively, 31.1 kcal/mol (**A**, Figure 3) and 28.3 kcal/mol (**C**, Figure S8). Based on the experimental results, the (*R*)-product should be formed in minor amounts (~7.5 % of the product),[33] which appears incompatible with the high barriers.

An analysis of the involved hydride transfer TSs of Mechanism **A** indicates that the (*R*)-TS experiences less charge stabilization than the preferred (*S*)-TS. At the *pro*-(*S*) TS, the interactions of the amido group with the Co center helps to stabilize the emerging negative chanrge on the substrate, whereas at the *pro*-(*R*) TS, such a stabilization is not possible. This observation led us to explore how explicit solvent, which has the potential to stabilize the evolving charges, would affect the computed barriers for mechanism **A**. To this end, a MeOH molecule was hydrogen-bonded to the NH group of the substrate, which was motivated by the X-ray structure of a Co(DuPhos)-methyl 2-acetamidoacrylate complex, where a solvent molecule (dimethyl ether) is bound to this NH.[2]

The DFT models used here cannot provide a reliable prediction of the energy of forming a hydrogen bond between a MeOH molecule from the bulk and the coordinated substrate, as the interactions of MeOH with the bulk cannot be computed, and the entropy of a free MeOH likely is overestimated. Therefore, for calculations of the free energy barriers in presence of an explicit MeOH, we have computed these relative to the Co(0)-Sub-species that has a hydrogen-bonded MeOH molecule. Interestingly, the hydrogen-bonded MeOH decreases the barriers for Mechanism **A** (Fig. 4 and S11). The decrease is slight for the (*S*)-pathway (1.4 kcal/mol), but significant for the (*R*)-pathway (7.1 kcal/mol), which we ascribe to improved charge stabilization. We emphasize that the inclusion of a solvent molecule brings with it computational complications, because many different conformations are possible, which would require dynamics to evaluate. Thus, the barriers obtained in presence of MeOH are to be viewed as approximate, however, they indicate that formation of the (*R*)-product via mechanism **A** is feasible under experimental conditions.

Also for mechanism **C**, a barrier reduction of up to 5 kcal/mol is observed, when explicit MeOH is added (SI, Figure S8). The proton transfer step is found to be rate limiting for both (*S*) and (*R*) pathways of mechanism **C**, with barriers of 20.9 and 23.4 kcal/mol, respectively. This implies that in presence of explicit solvent, the computed overall barrier for hydrogenation of methyl 2-acetamidoacrylate to the (*S*)-product via the metallacycle mechanism **C** (20.9 kcal/mol, Fig. S8) is two kcal/mol lower than via the redox mechanism **A** (22.9 kcal/mol, Figure 4), however, the difference is too small to definitely identify one of these mechanisms as preferred. It must be expected that the error of DFT on absolute barriers (e.g. the overall barrier for a mechanism) is larger than the error on relative barriers (e.g. the difference between two diastereomeric TSs from the same pathway). With a 2 kcal/mol difference between Mechanisms **A** and **C**, we conclude that both may possible and may be competing for hydrogenation of methyl 2-acetamidoacrylate. Importantly, both mechanisms appear viable at the reaction temperature of 323 K and in presence of explicit solvent, both mechanisms provide feasible barriers for formation of both the (*R*) and the (*S*) product.

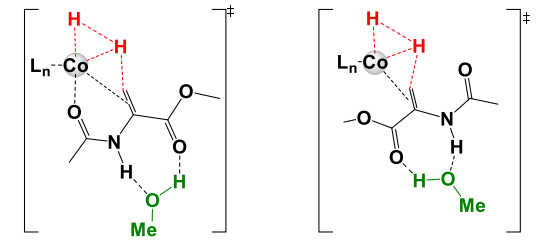

Figure 4. Optimized *pro*-(*S*) and -(*R*) hydride transfer TSs for Co-^{Ph}BPE-catalyzed hydrogenation of methyl 2-acetamidoacrylate via in Mechanism **A**, with and without a hydrogen-bonded MeOH (barriers relative to reactant with or without MeOH, respectively, kcal/mol, 323 K).

For mechanism **D**, the explicit solvent interactions do not change the barriers significantly (SI, Fig. S9). We also tested if MeOH could open other reaction patwhays, for example, coordinate to Co, while serving as a hydrogen bond donor, However, this raises the barriers significantly (SI, Fig. S12), making this possibility unfavorable. Coordinated MeOH could instead potentially function as a proton source. In this process, a Co-methoxy species is formed, whose regeneration has a barrier of 44.5 kcal/mol (SI, Fig. S13), excluding this pathway. This is in agreement with deuterium labelling studies that indicate that MeOH remains intact during hydrogenation [experimental result may be added].

We conclude that the solvent may play a vital role in hydrogen-bond stabilization during Co-^{Ph}BPE-catalyzed conversion of methyl 2-acetamidoacrylate via redox mechanism **A** and metallacycle mechanism **C**. A similar but much smaller effect of the explicit solvent is also observed for hydrogenation of *dehydro*-levetiracetam (Fig. S4, S14a and S14b). For this substrate, the barriers for formation of the (*S*)-product in presence of explicit solvent remain similar for Mechansim **A** and **C**, and thus also for this enamide, both mechanisms may contribute to the formation of the major product.

Enantioselectivity of Co-^{Ph}BPE-catalyzed hydrogenation of methyl 2-acetamidoacrylate and dehydro-levetiracetam: We evaluated the computed enantioselectivity of Co-^{Ph}BPE-catalyzed hydrogenation of methyl 2-acetamidoacrylate by using all TSs that correspond to the rate-limiting steps in the energetically close lying redox mechanism **A** (Figure 4) and the metallacylce mechanism **C** (SI, Fig. S8). In absence of explicit solvent, the barriers for the (*R*) product are high, implying an enatioselectivity of 99.8 % (*S*) should be observed (Table S2, SI). With explicit solvent, the barriers become more reasonable and the computed *e.e.* drops to 94.7 % (*S*), which is a slight overestimation compared to the experimentally reported *e.e.* of 85 % (*S*)[33] (323 K, Table 2). The results indicate that the two mechanisms can explain the enantioselectivity observed with this substrate. We note, however, that the computed values should be considered as approximate, because the precise location of the hydrogen bonded MeOH molecule is not possible to determine, and it is likely that multiple MeOHs are bound, whose computations, however, is beyond the possibilities of the static DFT methods employed here.

The enantioselectivity of the Co-^{Ph}BPE catalyzed asymmetric hydrogenation of *dehydro*-levetiracetam is also computed using all energetically close-lying TSs, including mechanism **A** (Figure S14a) and the 4 and 5-membered metallacycle mechanisms **C** (Figure S14b and S4, respectively). The obtained *e.e.* in absence of explicit solvent is 43.3 % (Table S1) which is much smaller than experiment, 98.3 % (*S*).[33] If MeOH is hydrogen-bonded to the substrate, the computed *e.e.* increases to 76.6 % (*S*) (Table 2). Interestingly, the experimental screening of solvents indicated a significant effect of the solvent on the observed enantioselectivity, with *e.e.* values varying from 76 to 94 % (*S*) at RT in different solvents (MeOH, EtOH, iPrOH, TFE).[33] This supports a role of explicit solvent interactions in determining the final enantiomeric excess. Such effects cannot be expected to be fully captured through including of a single explicit solvent molecule in the DFT calculations. However, our results indicate that if explicit solvent forms hydrogen bonds with the coordinated substrate, then this affects both the hydrogenation barriers and the resulting enantiomeric excesses.

Table 2. Computed free energy barriers (kcal/mol) and comparison of computed and experimental *e.e.*'s at 323 K for Co-^{Ph}BPE-catalyzed hydrogenation of two enamides.

Substrate	Barriers$_{comp}$[a]	*e.e.*$_{comp}$	*e.e.*$_{exp}$[b]
Methyl 2-acetamidoacrylate	*Mech.* ***A***[c] (S) 22.9 (*R*) 24.0 *Mech.* ***C****(6m)*[d] (*S*) 20.9 (*R*) 23.4	94.7% (*S*)	85.0% (*S*)
Dehydro-levetiracetam	*Mech.* ***A***[e] (*S*) 25.2 (*R*) 30.0 *Mech.* ***C****(5m)*[f] (*S*) 22.8 (*R*) 24.1 *Mech.* ***C****(4m)*[g] (*S*) 25.4 (*R*) 26.1	76.6% (*S*)	98.3% (*S*)

[a]With explicit MeOH, [b]From ref. [33], [c]Redox mechanism A, Fig. 4, [d]Non-redox metallacycle mechansism C via 6-membered metallcycle, Fig. S8, SI, [e]Redox mechanism A, Fig. S14a, SI, [f]Non-redox Mechanism C via 5-membered metallacyle, Fig. S4, SI, [g]Non-redox mechansism C via 4-membered metallacyle, Fig. S14b, SI.

CONCLUSIONS

We have investigated the intimate details of Co(0)-^{Ph}BPE-catalyzed hydrogenation of enamides. Two enamides were studied computationally, of which one contains an ionizable NH_2 group and the other an ionizable secondary amide (Table 1). Despite the large differences in the molecular structure of the two substrates and the plethora of putative hydrogenation mechanisms that are conceivable for these enamides (Scheme 1), our results suggest that both follow the same trend: For both, the computed barriers indicate that the preferred mechanism is a non-redox Co(II) metallacycle pathway (Mechanism **C**), but for both, the Co(0)/Co(II) redox pathway **A** is only slightly higher in energy and may be competing. A significant difference between the two substrates is the type of metallacycle intermediate that they form, with four- and five-membered metallacycles for *dehydro*-levetiracetam and six-membered metallacycles for methyl 2-acetamidoacrylate.

Our computationl work further shows that inclusion of an explicit MeOH solvent molecule in the computational models lowers critical barriers and is essential to obtain computed *e.e.*'s in line with experimental results. This result is supported by the experimentallly observed solvent-dependence of the enantiomeric excess.[33]

The overall results obtained for Co-catalyzed hydrogenation of enamides highlight the fact that non-precious metals may show highly complex mechanistic scenarios with competing redox and non-redox reaction pathways, which in addition may be significantly influenced by the solvent.

ASSOCIATED CONTENT

Supporting Information

The Supporting Information is available free of charge on the ACS Publications website:

- Optimized coordinates, which can be conveniently visualized with the Mercury program from the Cambridge Crystallographic Data Centre (XYZ file)
- Additional computational results as described in the text and experimental details (PDF)

AUTHOR INFORMATION

Corresponding Author: [email to be added]

ACKNOWLEDGMENT

This work has been supported by a Centre of Excellence Grant (No. 262695), by the Tromsø Research Foundation (No. TFS2016KHH), by Notur - The Norwegian Metacenter for Computational Science through grants of computer time (No. nn9330k and nn4654k), and by NordForsk (No. 85378).

REFERENCES

1. Vogiatzis, K. D.; Polynski, M. V.; Kirkland, J. K.; Townsend, J.; Hashemi, A.; Liu, C.; Pidko, E. A., Computational Approach to Molecular Catalysis by 3d Transition Metals: Challenges and Opportunities. *Chem. rev.* **2019,** *119* (4), 2453-2523.
2. Zhong, H.; Friedfeld, M. R.; Chirik, P. J., Syntheses and Catalytic Hydrogenation Performance of Cationic Bis(phosphine)Cobalt(I) Diene and Arene Compounds. *Angew. Chem. Int. Ed.* **2019,** *58* (27), 9194-9198.
3. Zhang, Z.; Butt, N. A.; Zhou, M.; Liu, D.; Zhang, W., Asymmetric Transfer and Pressure Hydrogenation with Earth-Abundant Transition Metal Catalysts. *Chin. J. Chem.* **2018,** *36* (5), 443-454.
4. Chan, A. S. C.; Pluth, J. J.; Halpern, J., Identification of the enantioselective step in the asymmetric catalytic hydrogenation of a prochiral olefin. *J. Am. Chem. Soc.* **1980,** *102* (18), 5952-5954.
5. Halpern, J., Mechanism and Stereoselectivity of Asymmetric Hydrogenation. *Science* **1982,** *217* (4558), 401.
6. Halpern, J., Mechanism and stereochemistry of asymmetric catalysis by metal complexes. *Pure. Appl. Chem.* **1983,** *55* (1), 99.
7. Verdolino, V.; Forbes, A.; Helquist, P.; Norrby, P.-O.; Wiest, O., On the mechanism of the rhodium catalyzed acrylamide hydrogenation. *J. Mol. Catal. A-Chem.* **2010,** *324* (1), 9-14.
8. Chirik, P. J.; Wieghardt, K., Radical Ligands Confer Nobility on Base-Metal Catalysts. *Science* **2010,** *327* (5967), 794-795.
9. Morello, G. R.; Zhong, H.; Chirik, P. J.; Hopmann, K. H., Cobalt-catalysed alkene hydrogenation: a metallacycle can explain the hydroxyl activating effect and the diastereoselectivity. *Chem. Sci.* **2018,** *9* (22), 4977-4982.
10. Arevalo, R.; Chirik,P. J., Enabling Two-Electron Pathways with Iron and Cobalt: From Ligand Design to Catalytic Applications. *J. Am. Chem. Soc.* **2019,** *141* (23), 9106-9123.
11. Casey, C. P.; Guan, H., An Efficient and Chemoselective Iron Catalyst for the Hydrogenation of Ketones. *J. Am. Chem. Soc.* **2007,** *129* (18), 5816-5817.
12. Casey, C. P.; Guan, H., Cyclopentadienone Iron Alcohol Complexes: Synthesis, Reactivity, and Implications for the Mechanism of Iron-Catalyzed Hydrogenation of Aldehydes. *J. Am. Chem. Soc.* **2009,** *131* (7), 2499-2507.
13. Yu, R. P.; Darmon, J. M.; Milsmann, C.; Margulieux, G. W.; Stieber, S. C. E.; DeBeer, S.; Chirik, P. J., Catalytic Hydrogenation Activity and Electronic Structure Determination of Bis(arylimidazol-2-ylidene)pyridine Cobalt Alkyl and Hydride Complexes. *J. Am. Chem. Soc.* **2013,** *135* (35), 13168-13184.
14. Bart, S. C.; Lobkovsky, E.; Chirik, P. J., Preparation and Molecular and Electronic Structures of Iron(0) Dinitrogen and Silane Complexes and Their Application to Catalytic Hydrogenation and Hydrosilation. *J. Am. Chem. Soc.* **2004,** *126* (42), 13794-13807.
15. Rösler, S.; Obenauf, J.; Kempe, R., A Highly Active and Easily Accessible Cobalt Catalyst for Selective Hydrogenation of C═O Bonds. *J. Am. Chem. Soc.* **2015,** *137* (25), 7998-8001.
16. Yu, R. P.; Darmon, J. M.; Hoyt, J. M.; Margulieux, G. W.; Turner, Z. R.; Chirik, P. J., High-Activity Iron Catalysts for the Hydrogenation of Hindered, Unfunctionalized Alkenes. *Acs. Catal.* **2012,** *2* (8), 1760-1764.
17. Tokmic, K.; Markus, C. R.; Zhu, L.; Fout, A. R., Well-Defined Cobalt(I) Dihydrogen Catalyst: Experimental Evidence for a Co(I)/Co(III) Redox Process in Olefin Hydrogenation. *J. Am. Chem. Soc.* **2016,** *138* (36), 11907-11913.
18. Zhang, G.; Scott, B. L.; Hanson, S. K., Mild and Homogeneous Cobalt-Catalyzed Hydrogenation of C=C, C=O, and C=N Bonds. *Angew. Chem. Int. Ed.* **2012,** *51* (48), 12102-12106.
19. Zhang, G.; Vasudevan, K. V.; Scott, B. L.; Hanson, S. K., Understanding the Mechanisms of Cobalt-Catalyzed Hydrogenation and Dehydrogenation Reactions. *J. Am. Chem. Soc.* **2013,** *135* (23), 8668-8681.
20. Lin, T.-P.; Peters, J. C., Boryl-Mediated Reversible H_2 Activation at Cobalt: Catalytic Hydrogenation, Dehydrogenation, and Transfer Hydrogenation. *J. Am. Chem. Soc.* **2013,** *135* (41), 15310-15313.
21. Elangovan, S.; Topf, C.; Fischer, S.; Jiao, H.; Spannenberg, A.; Baumann, W.; Ludwig, R.; Junge, K.; Beller, M., Selective Catalytic Hydrogenations of Nitriles, Ketones, and Aldehydes by Well-Defined Manganese Pincer Complexes. *J. Am. Chem. Soc.***2016,** *138* (28), 8809-8814.
22. Adam, R.; Bheeter, C. B.; Cabrero-Antonino, J. R.; Junge, K.; Jackstell, R.; Beller, M., Selective Hydrogenation of Nitriles to Primary Amines by using a Cobalt Phosphine Catalyst. *Chem. Sus. Chem.* **2017,** *10* (5), 842-846.
23. Ganguly, G.; Malakar, T.; Paul, A., Theoretical Studies on the Mechanism of Homogeneous Catalytic Olefin Hydrogenation and Amine–Borane Dehydrogenation by a Versatile Boryl-Ligand-Based Cobalt Catalyst. *Acs. Catal.* **2015,** *5* (5), 2754-2769.
24. Knijnenburg, Q.; Horton, A. D.; Heijden, H. v. d.; Kooistra, T. M.; Hetterscheid, D. G. H.; Smits, J. M. M.; Bruin, B. d.; Budzelaar, P. H. M.; Gal, A. W., Olefin hydrogenation using diimine pyridine complexes of Co and Rh. *J. Mol. Catal. A-Chem.* **2005,** *232* (1), 151-159.
25. Li, L.; Lei, M.; Sakaki, S., DFT Mechanistic Study on Alkene Hydrogenation Catalysis of Iron Metallaboratrane: Characteristic Features of Iron Species. *Organometallics* **2017,** *36* (18), 3530-3538.
26. Van Putten, R.; Uslamin, E. A.; Garbe, M.; Liu, C.; Gonzalez-de-Castro, A.; Lutz, M.; Junge, K.; Hensen, E. J. M.; Beller, M.; Lefort, L.; Pidko, E. A., Non-Pincer-Type Manganese Complexes as Efficient Catalysts for the Hydrogenation of Esters. *Angew. Chem. Int. Ed.* **2017,** *56* (26), 7531-7534.

27. Zhang, Z.; Li, Y.; Hou, C.; Zhao, C.; Ke, Z., DFT study of CO_2 hydrogenation catalyzed by a cobalt-based system: an unexpected formate anion-assisted deprotonation mechanism. *Catal. Sci.* **2018,** *8* (2), 656-666.
28. Hou, C.; Li, Y.; Zhao, C.; Ke, Z., A DFT study of Co(i) and Ni(ii) pincer complex-catalyzed hydrogenation of ketones: intriguing mechanism dichotomy by ligand field variation. *Catal. Sci*. **2019,** *9* (1), 125-135.
29. Friedfeld, M. R.; Margulieux, G. W.; Schaefer, B. A.; Chirik, P. J., Bis(phosphine)cobalt Dialkyl Complexes for Directed Catalytic Alkene Hydrogenation. *J. Am. Chem. Soc.* **2014,** *136* (38), 13178-13181.
30. Zhong, H.; Friedfeld, M. R.; Camacho-Bunquin, J.; Sohn, H.; Yang, C.; Delferro, M.; Chirik, P. J., Exploring the Alcohol Stability of Bis(phosphine) Cobalt Dialkyl Precatalysts in Asymmetric Alkene Hydrogenation. *Organometallics* **2019,** *38* (1), 149-156.
31. Monfette, S.; Turner, Z. R.; Semproni, S. P.; Chirik, P. J., Enantiopure C1-Symmetric Bis(imino)pyridine Cobalt Complexes for Asymmetric Alkene Hydrogenation. *J. Am. Chem. Soc.* **2012,** *134* (10), 4561-4564.
32. Hopmann, K. H., Cobalt–Bis(imino)pyridine-Catalyzed Asymmetric Hydrogenation: Electronic Structure, Mechanism, and Stereoselectivity. *Organometallics* **2013,** *32* (21), 6388-6399.
33. Friedfeld, M. R.; Zhong, H.; Ruck, R. T.; Shevlin, M.; Chirik, P. J., Cobalt-catalyzed asymmetric hydrogenation of enamides enabled by single-electron reduction. *Science* **2018,** *360* (6391), 888-893.
34. Chen, J.; Chen, C.; Ji, C.; Lu, Z., Cobalt-Catalyzed Asymmetric Hydrogenation of 1,1-Diarylethenes. *Org. Lett.* **2016,** *18* (7), 1594-1597.
35. Smith, S. A. M.; Lagaditis, P. O.; Lüpke, A.; Lough, A. J.; Morris, R. H., Unsymmetrical Iron P-NH-P′ Catalysts for the Asymmetric Pressure Hydrogenation of Aryl Ketones. *Chem. Eur.* **2017,** *23* (30), 7212-7216.
36. Seo, C. S. G.; Morris, R. H., Catalytic Homogeneous Asymmetric Hydrogenation: Successes and Opportunities. *Organometallics* **2019,** *38* (1), 47-65.
37. Zhou, S.; Fleischer, S.; Junge, K.; Das, S.; Addis, D.; Beller, M., Enantioselective Synthesis of Amines: General, Efficient Iron-Catalyzed Asymmetric Transfer Hydrogenation of Imines. *Angew. Chem. Int.l Ed.* **2010,** *49* (44), 8121-8125.
38. Sonnenberg, J. F.; Wan, K. Y.; Sues, P. E.; Morris, R. H., Ketone Asymmetric Hydrogenation Catalyzed by P-NH-P′ Pincer Iron Catalysts: An Experimental and Computational Study. *Acs. Catal.* **2017,** *7* (1), 316-326.
39. Friedfeld, M. R.; Shevlin, M.; Margulieux, G. W.; Campeau, L.-C.; Chirik, P. J., Cobalt-Catalyzed Enantioselective Hydrogenation of Minimally Functionalized Alkenes: Isotopic Labeling Provides Insight into the Origin of Stereoselectivity and Alkene Insertion Preferences. *J. Am. Chem. Soc.* **2016,** *138* (10), 3314-3324.
40. Knowles, W. S.; Sabacky, M. J.; Vineyard, B. D.; Weinkauff, D. J., Asymmetric hydrogenation with a complex of rhodium and a chiral bisphosphine. *J. Am. Chem. Soc.* **1975,** *97* (9), 2567-2568.
41. Kitamura, M.;Tsukamoto,M.; Bessho, Y.; Yoshimura, M.; Kobs, U.; Widhalm, M.; Noyori, R., Mechanism of Asymmetric Hydrogenation of α-(Acylamino)acrylic Esters Catalyzed by BINAP−Ruthenium(II) Diacetate. *J. Am. Chem. Soc.* **2002,** *124* (23), 6649-6667.
42. Ma, X.; Lei, M., Mechanistic Insights into the Directed Hydrogenation of Hydroxylated Alkene Catalyzed by Bis-(phosphine)cobalt Dialkyl Complexes. *J. Org. Chem.* **2017,** *82* (5), 2703-2712.
43. Hopmann, K.H.; Bayer, A., On the Mechanism of Iridium-Catalyzed Asymmetric Hydrogenation of Imines and Alkenes: A Theoretical Study. *Organometallics* **2011,** *30* (9), 2483-2497.
44. Tutkowski, B.; Kerdphon, S.; Limé, E.; Helquist, P.; Andersson, P. G.; Wiest, O.; Norrby, P.-O., Revisiting the Stereodetermining Step in Enantioselective Iridium-Catalyzed Imine Hydrogenation. *Acs. Catal.* **2018,** *8* (1), 615-623.
45. Hu, Y.; Zhang, Z.; Zhang, J.; Liu, Y.; Gridnev, I. D.; Zhang, W., Cobalt-Catalyzed Asymmetric Hydrogenation of C=N Bonds Enabled by Assisted Coordination and Nonbonding Interactions. *Angew. Chem. Int. Ed.* **2019,** *58* (44), 15767-15771.
46. Gaussian 09, Revision D.01, Frisch M.J., Trucks G.W, Schlegel H.B., Scuseria G.E, Robb M.A., Cheesman J.R, Scalmani G., Barone V., Menucci B., Petersson G.A., Nakatsuji H., Caricato M., Li X., Hratchain H.P., Izmaylov A.F, Bloino J., Zheng G., Sonnenberg J.L, Hada M., Ehara M., Toyota K., Fukada R., Hasegawa J., Ishida M., Nakajima T., Honda Y., Kitao O., Nakai H., Vreven T., Montgomery J.A, Jr.,Peralta J.E., Ogliario F., Bearpark M., Heyd J.J., Brothers E., Kudin K.N., Staroverov V.N., Kobayashi R., Normand J., Raghavachari K. Rendell A., Burant J.C., Iyengar S.S., Tomasi J. , Cossi M., Rega N., Millam J.M,Klene M., Knox J.E., Cross J.B.,Bakken V., Adamo C., Jaramillo J., Gomperts R, Stratmann R.E.,Yazyev O., Austin A.J., Cammi R. Pomelli C., Ochterski J.W. , Martin R.L., Morokuma K., Zakrzewski V.G., Voth G.A., Salvador P., Dannenberg J.J, Dapprich S., Daniels, A.D., Farkas Ö., Foresman J.B., Ortiz J.V., Cioslowski J., Fox D.J. Gaussian, Inc., Wallingford CT, **2009.**
47. Grimme, S.; Antony, J.; Ehrlich, S.; Krieg, H., A consistent and accurate ab initio parametrization of density functional dispersion correction (DFT-D) for the 94 elements H-Pu. *J. Chem. Phys.* **2010,** *132* (15), 154104.
48. Tomasi, J.; Mennucci, B.; Cancès, E., *J. Mol. Struct-Theochem.* **1999,** *464*, 211.
49. Tomasi, J.; Mennucci, B.; Cammi, R., Quantum mechanical continuum solvation models. *Chem. Rev.* **2005,** *105* (8), 2999-3093.
50. Hopmann, K. H., How Accurate is DFT for Iridium-Mediated Chemistry? *Organometallics* **2016,** *35* (22), 3795-3807.
51. Hopmann, K.H., Quantum Chemical Studies of Asymmetric Reactions: Historical Aspects and Recent Examples. *Int. J. Quantum. Chem.* **2015,** *115* (18), 1232-1249.
52. The coordination mode cannot be expected to be the same due to a different charge and spin state (S=0) for the cationic species, S=1/2 here.
53. Ryu, H.; Park, J.; Kim, H. K.; Park, J. Y.; Kim, S.-T.; Baik, M.-H., Pitfalls in Computational Modeling of Chemical Reactions and How To Avoid Them. *Organometallics* **2018,** *37* (19), 3228-3239.
54. This is based on the assumption that H_2 coordination is not rate-limiting. Our attempts to find the TS-H_2 for this pathway were unsuccessful. However, calculations of the redox pathways for methyl 2-acetamidoacrylate show low barriers of 10.0 kcal/mol and 11.3 kcal/mol for H_2 coordination (Figure 3)

Supporting Information (Draft)

Mechanistic study of asymmetric Co-catalyzed hydrogenation of enamides

Ljiljana Pavlovic,[a] Hongyu Zhong,[b] Paul J. Chirik,[b] Kathrin H. Hopmann[a]

[a]Hylleraas Centre for Quantum Molecular Sciences, Department of Chemistry, UiT The Arctic University of Norway, N-9037 Tromsø, Norway
[b]Department of Chemistry, Princeton University, New Jersey 08544, United States.

Corresponding Author: [email to be added]

Contents

1. Evaluation of the Co-Substrate interaction strength

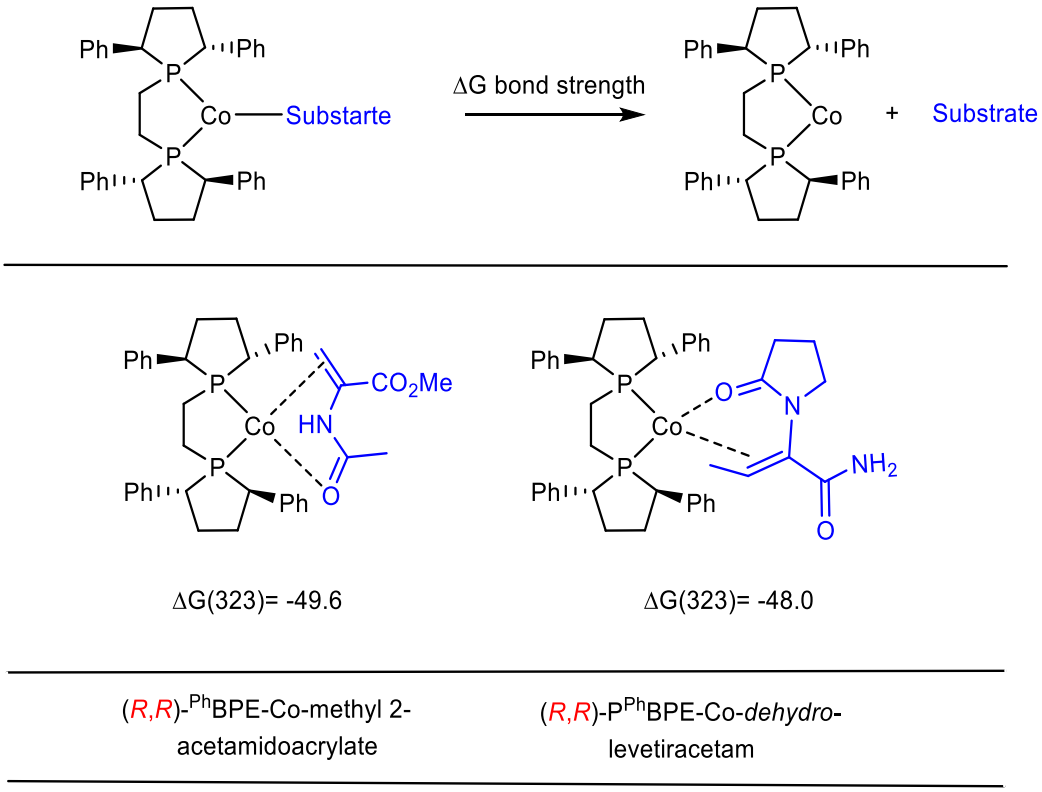

Figure S1. Computation of Co-Substrate interaction strength. Both enamides bind strongly to the cobalt-BPE complex. Free energies are given in kcal/mol.

2. Alternative mechanisms for the hydrogenation of *dehydro*-levetiracetam

2.1 Redox Co(0)-Co(II) mechanism A for the hydrogenation of *dehydro*-levetiracetam

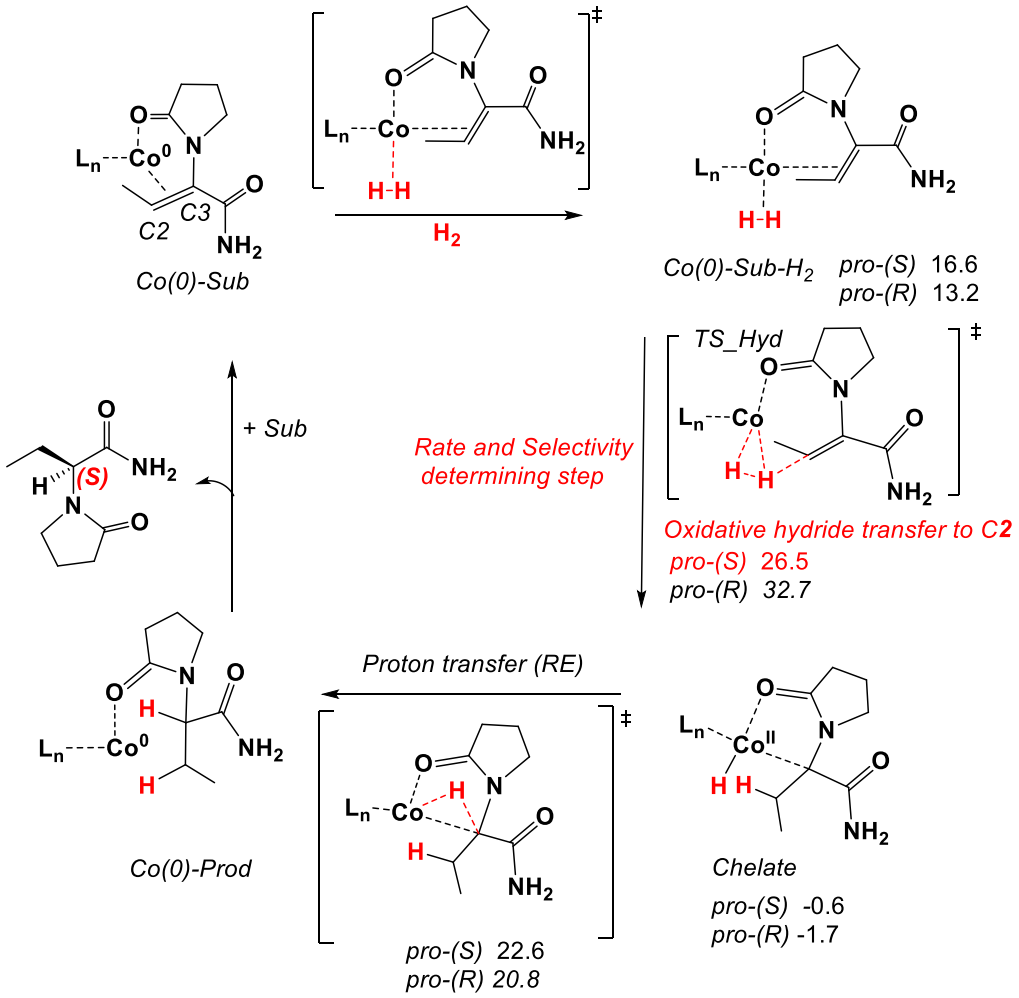

Figure S2. Mechanism and computed free energies (kcal/mol, 323 K, relative to Co-Sub) for Co-^{Ph}BPE-catalyzed hydrogenation of *dehydro*-levetiracetam via redox mechanism **A**, where oxidative hydride transfer occurs to the C2 atom via TS-Hyd. This step is rate-limiting for this mechanism, with a barrier of 26.5 kcal/mol for the formation of the (*S*)-product. In the final step, reductive elimination occurs in order to liberate the product and regenerate the catalyst. This step has a barrier of 23.2 kcal/mol for the (*S*)-pathway, assuming that the (*R*) and (*S*) intermediates are not in equilibrium (due to the high backwards barrier), and 24.3 kcal/mol if they are assumed to be in equilibrium.

2.2 Alternative non-redox σ-bond metathesis mechanism B for the hydrogenation of *dehydro*-levetiracetam

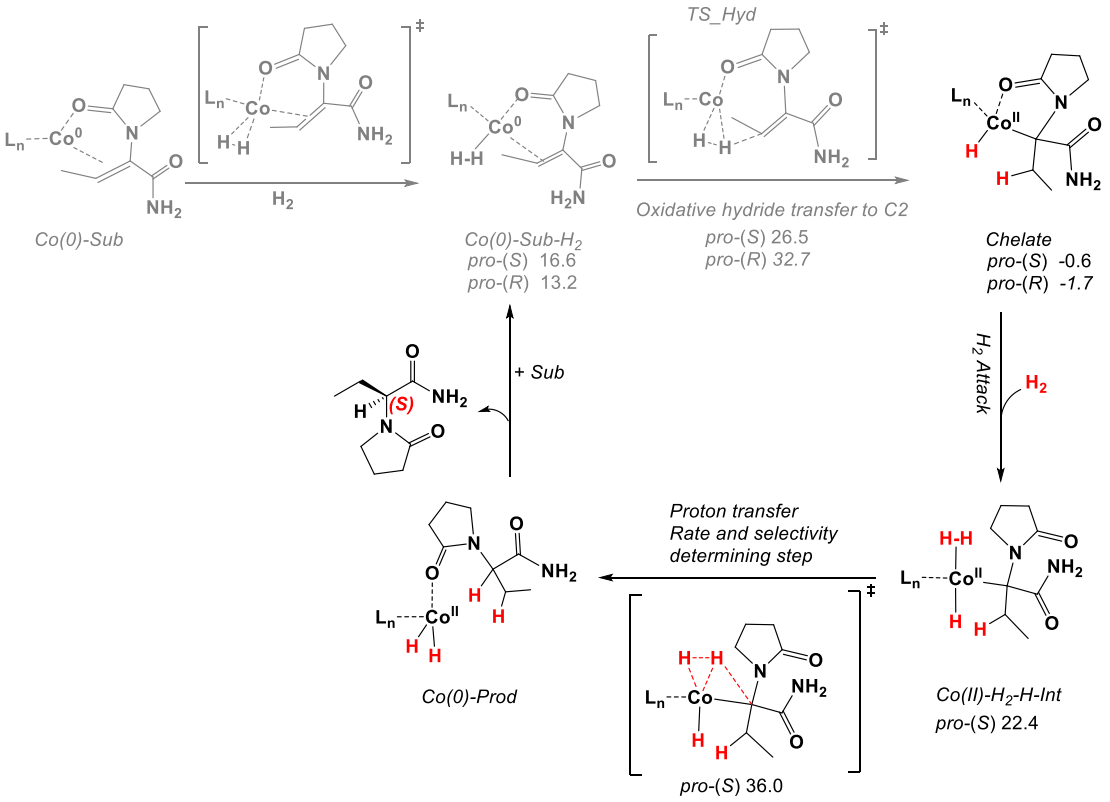

Figure S3. Mechanism and computed free energies (kcal/mol, 323 K, relative to Co-Sub) for Co-^{Ph}BPE-catalyzed hydrogenation of *dehydro*-levetiracetam via the non-redox σ-metathesis mechanism **B**. After formation of chelate intermediate, coordination of H_2 occurs, followed by a proton transfer step, which is found to be the rate- and selectivity-determining step. The overall barrier for the formation of the (*S*)-product is 37.7 kcal/mol.

2.3 Alternative metallacycle mechanism C for the hydrogenation of *dehydro*-levetiracetam with hydride transfer to C3 (5-membered metallacycle)

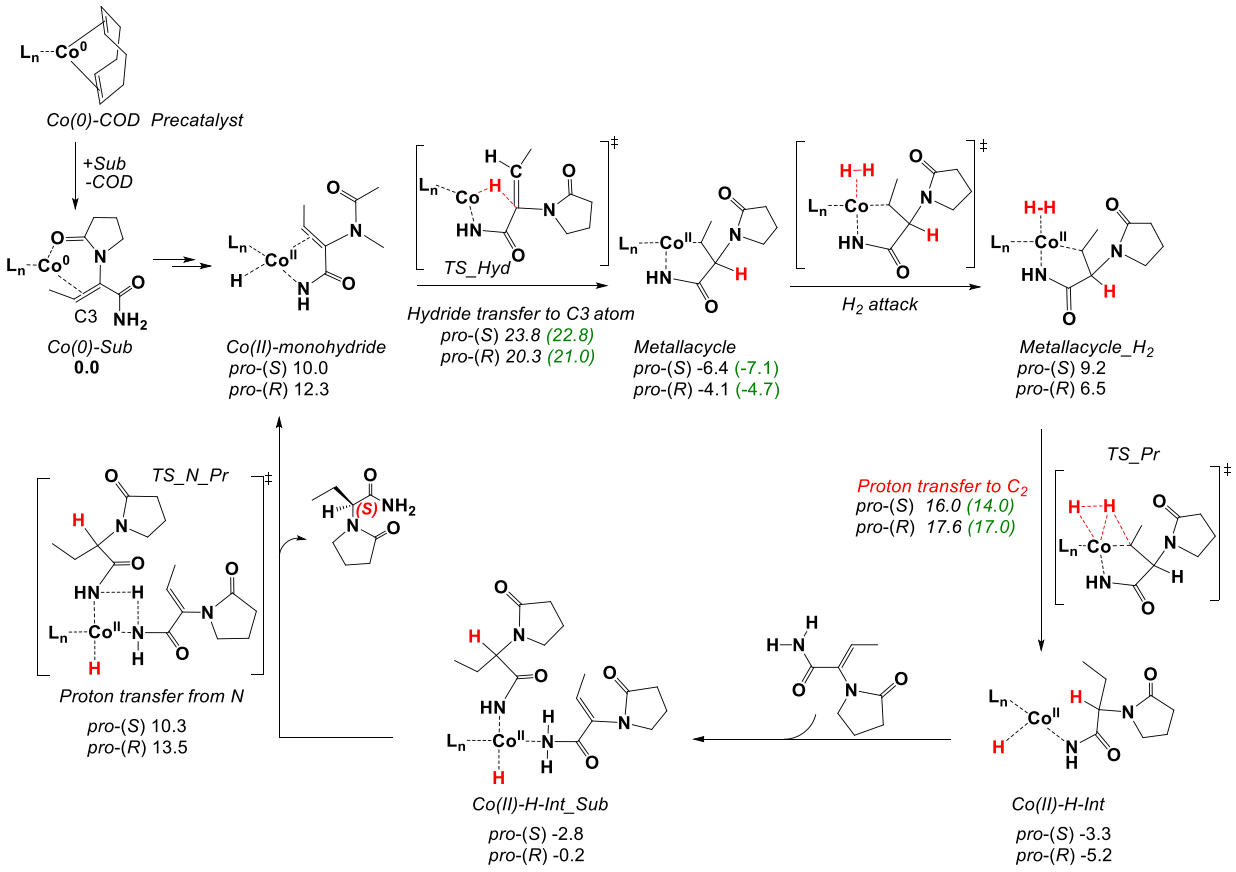

Figure S4. Mechanism and computed free energies (kcal/mol, 323 K, relative to Co-Sub) for Co-^{Ph}BPE-catalyzed hydrogenation of *dehydro*-levetiracetam via an alternative 5-membered metallacycle mechanism **C** where hydride transfer to the C3 atom occurs first. The barriers for this step are 20.3 kcal/mol and 23.8 kcal/mol, for pro-(*R*) and pro-(*S*) TSs, respectively. Then, H_2 coordination takes place, followed by proton transfer to the C2 atom in order to form the Metallacycle-H_2 intermediate. The computed barriers for this step are 22.4 kcal/mol and 24.0 kcal/mol for pro-(*S*) and pro-(*R*) TS structures. Finally, coordination of another substrate occurs, which transfers its proton to the nitrogen atom, resulting in the final product and the regeneration of the active Co(II)-monohydride species. The rate-limiting step for the formation of (*S*)-product is hydride transfer (23.8 kcal/mol), whereas for the formation of (*R*)-product it is proton transfer step (24.0 kcal/mol). Energies in parenthesis with green colour are from computational models including an explicit solvent molecule hydrogen-bonded to the substrate.

3. A direct oxidative addition of the ionizable group of the substrate to Co(0)

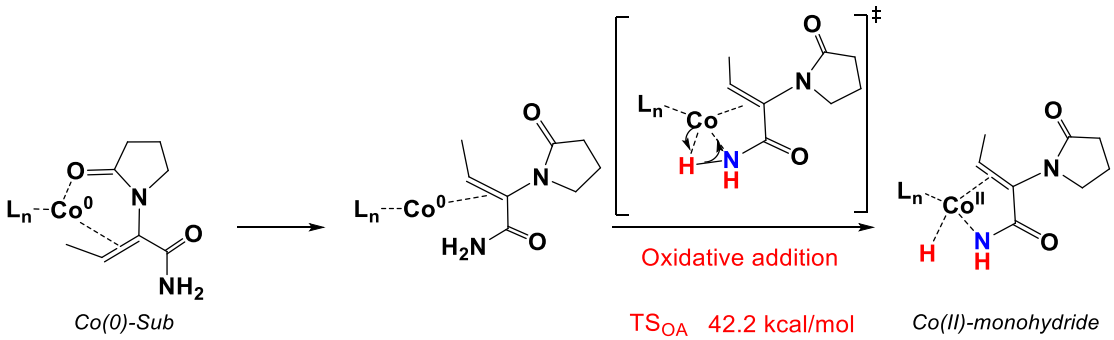

Figure S5. Direct oxidative addition of the substrate (*dehydro*-levetiracetam) to convert Co(0)-Sub to a Co(II)-monohydride intermediate via transition state TS_{OA}. The free energy barrier of 42.2 kcal/mol is given relative to Co(0)-Sub and is not feasible at the experimental temperature (323 K), indicating that the Co(II)-monohydride intermediate cannot be formed through direct oxidative addition. An alternative pathway is described in the main text.

4. Alternative mechanisms for the hydrogenation of methyl 2-acetamidoacrylate

4.1 Alternative redox Co(0)-Co(II) mechanism A of methyl 2-acetamidoacrylate with hydride transfer to the C2 atom

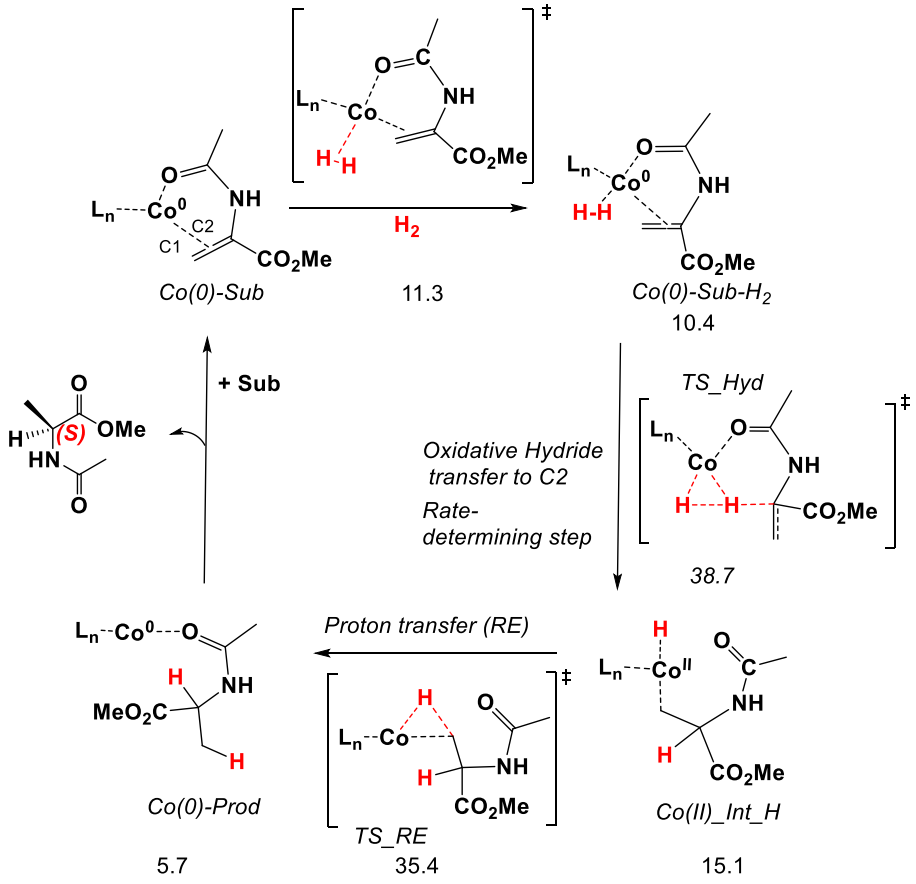

Figure S6. Mechanism and computed free energies (kcal/mol, 323 K, relative to Co-Sub) for Co-^{Ph}BPE-catalyzed hydrogenation of methyl 2-acetamidoacrylate via an alternative redox mechanism **A** where oxidative hydride transfer occurs to the C2 atom via TS-Hyd (compared to C1 in the main text). This step is found to be rate-limiting with a barrier of 38.7 kcal/mol. Evaluated is only the reaction pathway that will give (*S*)-product.

4.2 Alternative non-redox σ-bond metathesis mechanism B for methyl 2-acetamidoacrylate; hydride transfer to C1

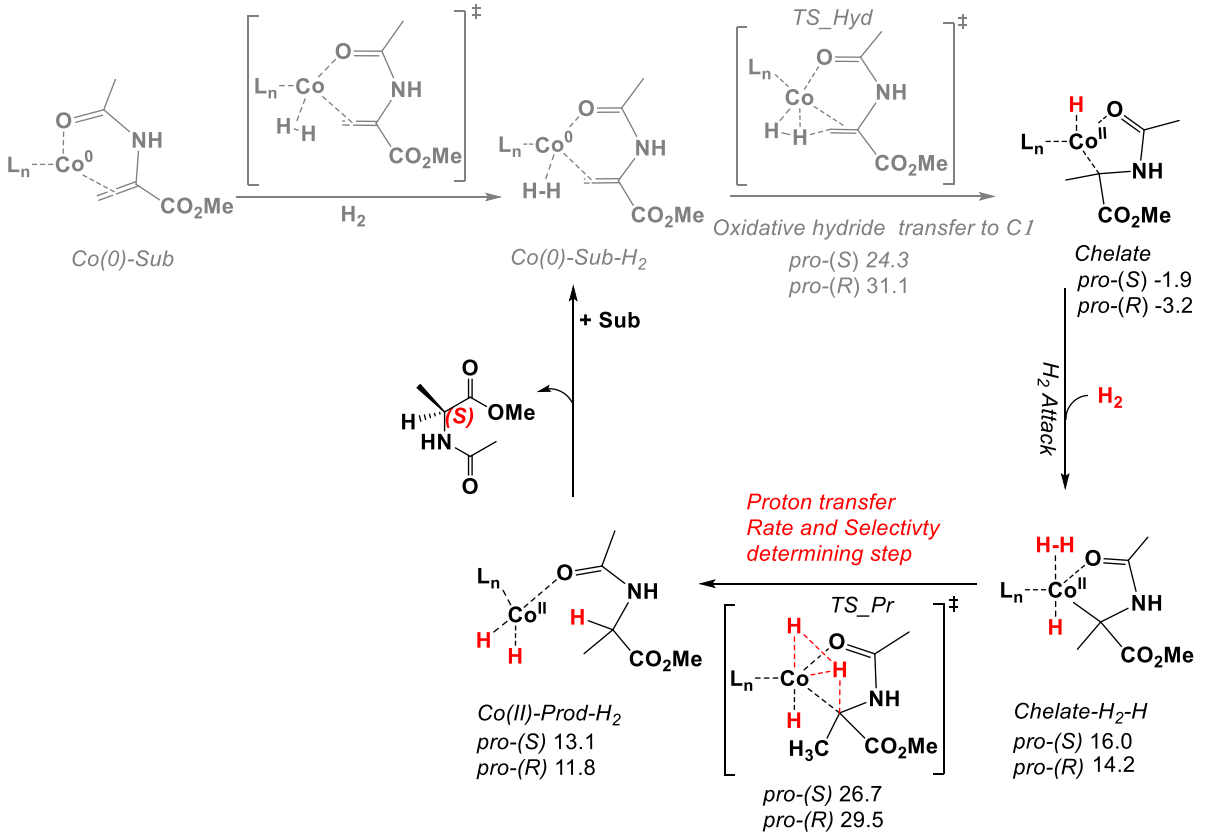

Figure S7. Mechanism and computed free energies (kcal/mol, 323 K, relative to Co-Sub) for Co-^{Ph}BPE-catalyzed hydrogenation of methyl 2-acetamidoacrylate via a non-redox σ-metathesis mechanism **B**, in which after formation of chelate intermediate, coordination of H_2 occurs, followed by proton transfer step, which is found to be the rate- and selectivity determining step. The overall barrier for the formation of the (*R*)-product is 32.7 kcal/mol and 28.6 kcal/mol for the (*S*)-product (for the latter assuming the chelate intermediates are not in equilibrium, if they are, the (*S*)-barrier increases to 29.9 kcal/mol).

4.3 Alternative non-redox mechanism C for methyl 2-acetamidoacrylate, hydride transfer to C2

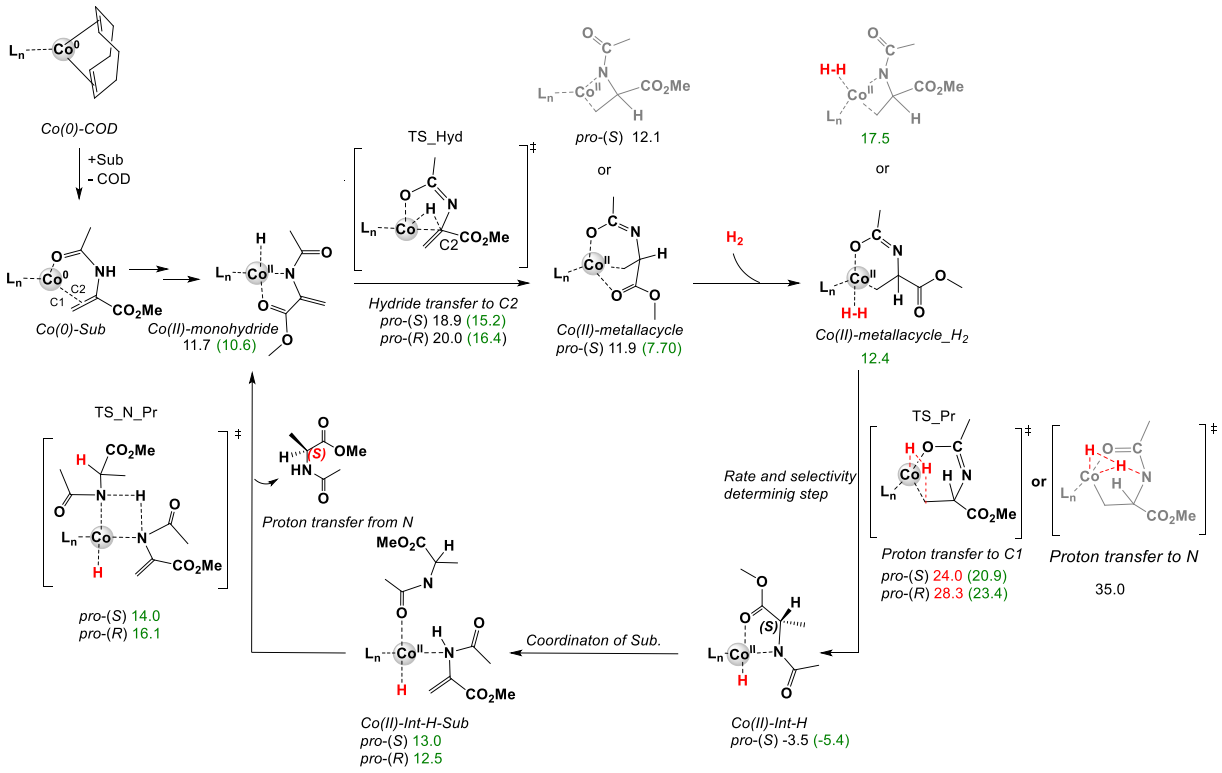

Figure S8. Mechanism and computed free energies (kcal/mol, 323 K, relative to Co-Sub) for Co-^{Ph}BPE-catalyzed hydrogenation of methyl 2-acetamidoacrylate via mechanism **C** where hydride transfer occurs to the **C2** atom. Note that the Co(II)-metallacycle and Co(II)-metallacycle-H_2 intermediate can adopt two conformations, where either the oxygen of the amido group or nitrogen of the amido group interacts with Cobalt. The barriers are 18.9 kcal/mol and 20.0 kcal/mol, for the pro-(*S*) and pro-(*R*) TSs. In the next step, either proton transfer to N or to C1 might occur. The barriers are 35 kcal/mol and 24.0 kcal/mol, respectively.

We also tested if addition of an explicit MeOH molecule that hydrogen bonds to the substrate changes the barriers of mechanism **C** (Energies in parenthesis with green colour are from computational models including an explicit solvent molecule hydrogen-bonded to the substrate). A significant effect of the explicit solvent on the barriers is observed. In presence of explicit MeOH, the rate-limiting step is the proton transfer, with barriers of 20.9 kcal/mol and 23.4 kcal/mol, for the pro-(*S*) and pro-(*R*) TSs, respectively.

4.4 Alternative imine mechanism D for methyl 2-acetoamidacrylate

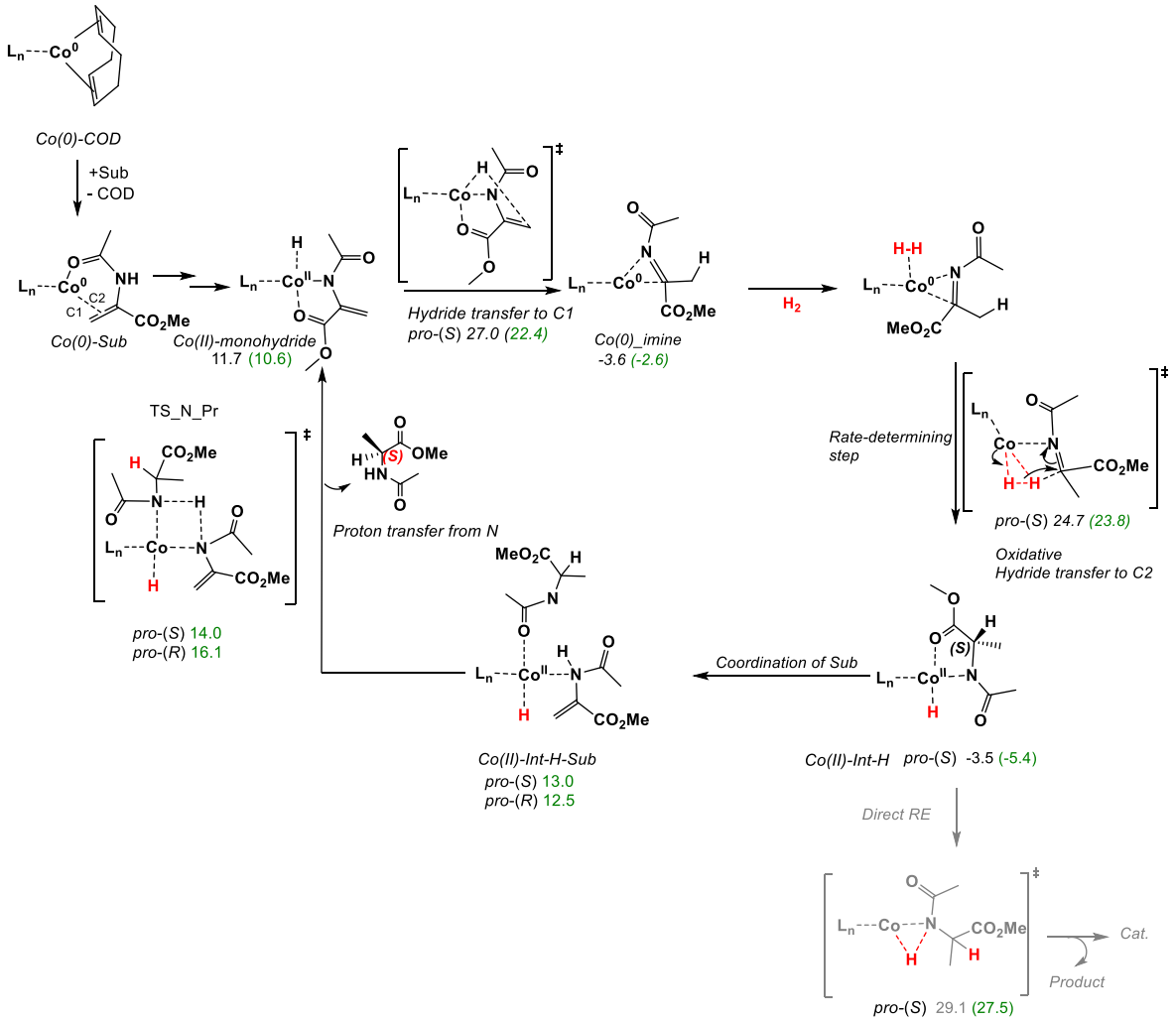

Figure S9. Mechanism and computed free energies (kcal/mol, 323 K, relative to Co-Sub) for Co-^{Ph}BPE-catalyzed hydrogenation of methyl 2-acetamidoacrylate via an alternative imine mechanism **D** in which enamine-imine tautomerization is expected to occur. (Hydride transfer to C1 has a barrier of 27.0 kcal/mol, with the explicit MeOH-Substrate interaction, this is reduced to 22.4 kcal/mol).Then, H_2 attack is followed by hydride transfer from H_2 to C2 atom to form the Co(II)-Int-H. The overall barrier is 28.3 kcal/mol (*S*-product), with MeOH hydrogen bonded to the substrate it is 26.4 kcal/mol. Energies in parenthesis with green colour are from computational models including an explicit solvent molecule hydrogen-bonded to the substrate

There is an alternative mechanism where after formation of the Co(II)-monohydride-H species direct reductive elimination might occur. However, the overall barrier is 32.7 kcal/mol. With MeOH hydrogen bonded to the MAA, a similar barrier of 32.9 kcal/mol is obtained. Only the reaction path that lead to the (*S*)-product was evaluated.

4.5 Alternative imine mechanism D-2 for methyl 2-acetamidoacrylate with heterolytic H_2 cleavage

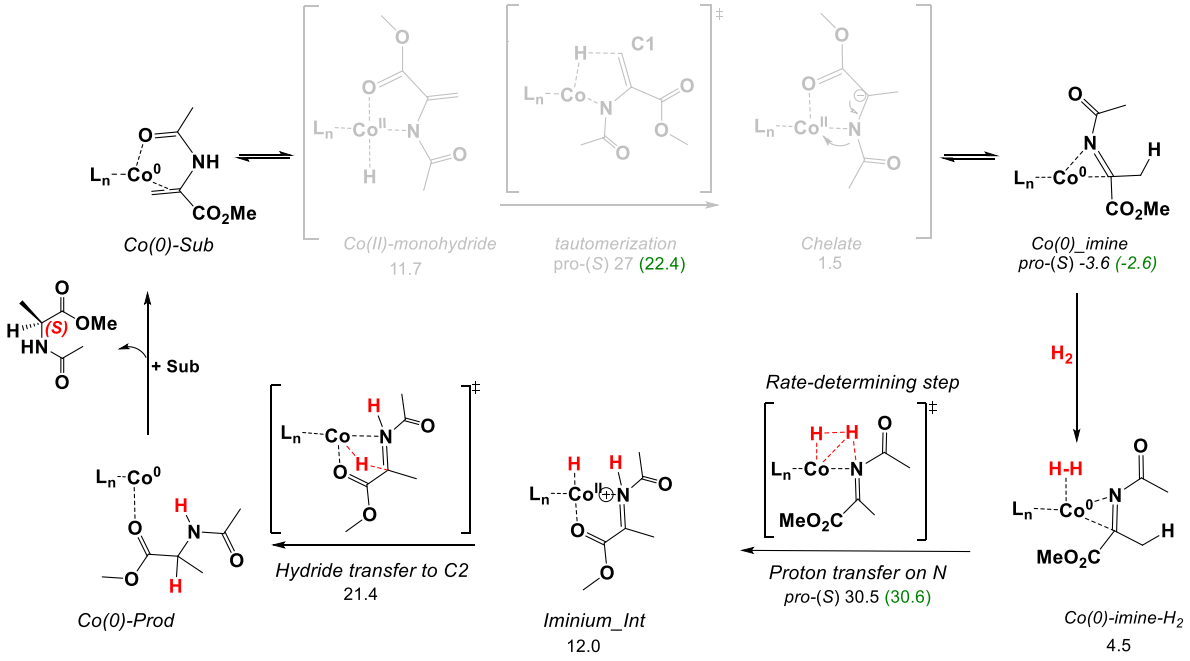

Figure S10. Mechanism and computed free energies (kcal/mol, 323 K, relative to Co-Sub) for Co-^{Ph}BPE-catalyzed hydrogenation of methyl 2-acetamidoacrylate via an alternative imine mechanism, where after H_2 coordination, proton transfer from H_2 on N atom takes place to form an iminium intermediated. This step is found to be rate-limiting with an overall barrier of 34.0 kcal/mol (computed relative to the imine). After proton transfer on N, hydride transfer on C2 atom occurs in order to liberate the product. The overall barrier with the explicit MeOH-Substrate interaction is 33.2 kcal/mol. Energies in parenthesis with green colour are from computational models including an explicit solvent molecule hydrogen-bonded to the substrate

4.6 Alternative mechanism A for methyl 2-acetamidoacrylate with MeOH as hydrogen bond donor to the substrate

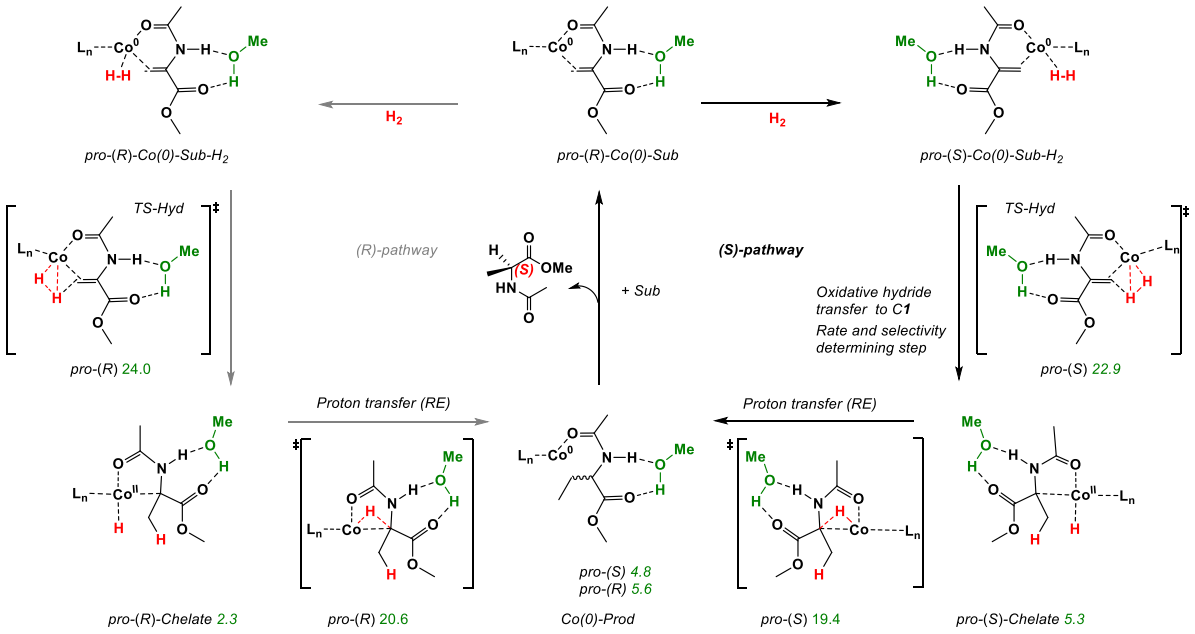

Figure S11. Mechanism and computed free energies (kcal/mol, 323 K, relative to Co-Sub) for Co-^{Ph}BPE-catalyzed hydrogenation of methyl 2-acetamidoacrylate via an alternative redox mechanism **A**, with MeOH as a hydrogen bond donor to the substrate. Evaluated are both pro-(*S*) and pro-(*R*) reaction pathways. In the first step, oxidative hydride transfer occurs to the C1 atom via pro-(*S*) and pro-(*R*) TS-Hyd structures to from the corresponding chelate intermediates. In the presence of MeOH (Energies are given with green colour), the barrier for the pro-(*S*) TS-Hyd is 22.9 kcal/mol, whereas the barrier for the pro-(*R*) TS-Hyd is 24.0 kcal/mol. This step is found to be rate-limiting. In the next step, the reductive elimination occurs through pro-(*S*) and pro-(*R*) TS_Pr structures with barriers of 19.4 kcal/mol and 20.6 kcal/mol, respectively.

4.7 Alternative mechanism A for methyl 2-acetamidoacrylate with one MeOH molecule coordinated to Co

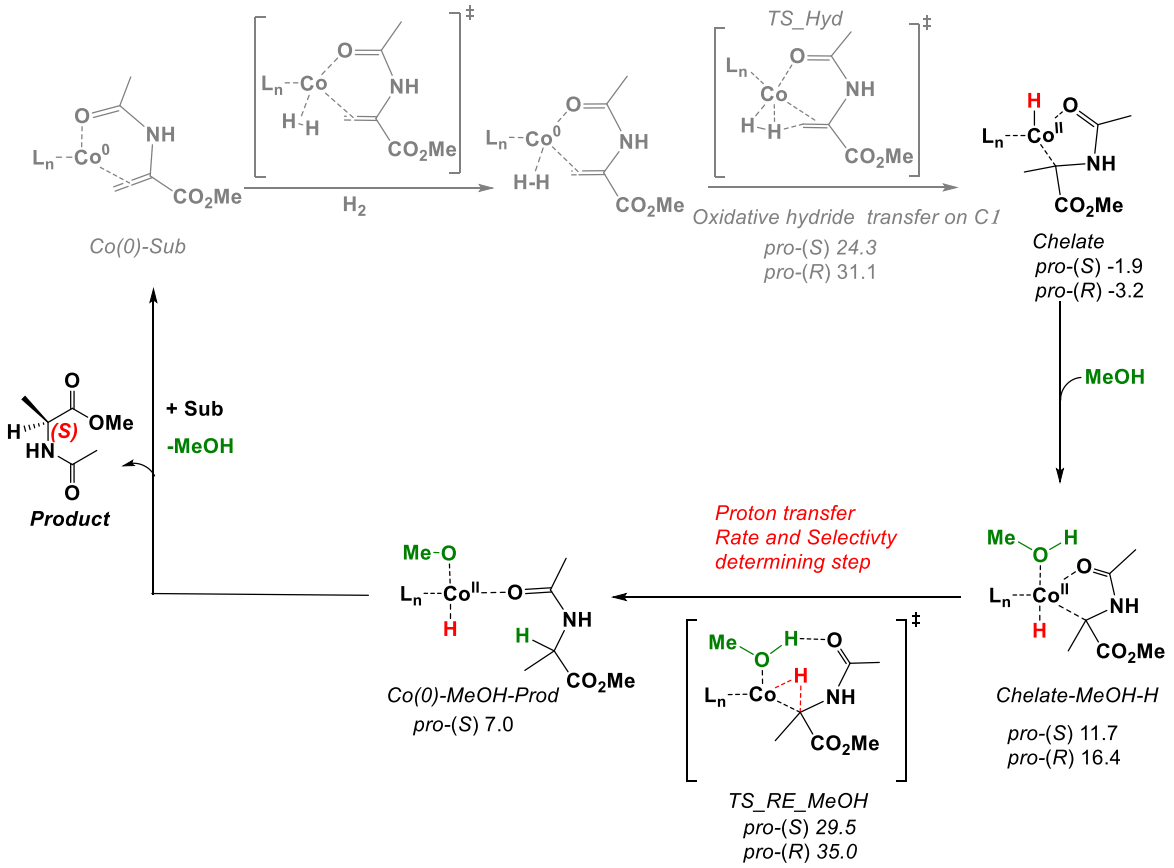

Figure S12. Mechanism and computed free energies (kcal/mol, 323 K, relative to Co-Sub) for Co-^{Ph}BPE-catalyzed hydrogenation of methyl 2-acetamidoacrylate via an alternative MeOH mechanism in which after formation of chelate intermediate, coordination of MeOH occurs. In the next step, reductive elimination takes place, while MeOH is coordinated to the metal centre. The overall barrier for the formation of (*S*)-product is 31.4 kcal/mol and for the (*R*)-product 38.2 kcal/mol, which is not feasible. The barriers were computed assuming that the (*R*) and (*S*) intermediates are not in equilibrium (due to the high backwards barrier).

4.8 Alternative mechanism for methyl 2-acetamidoacrylate with MeOH as proton donor

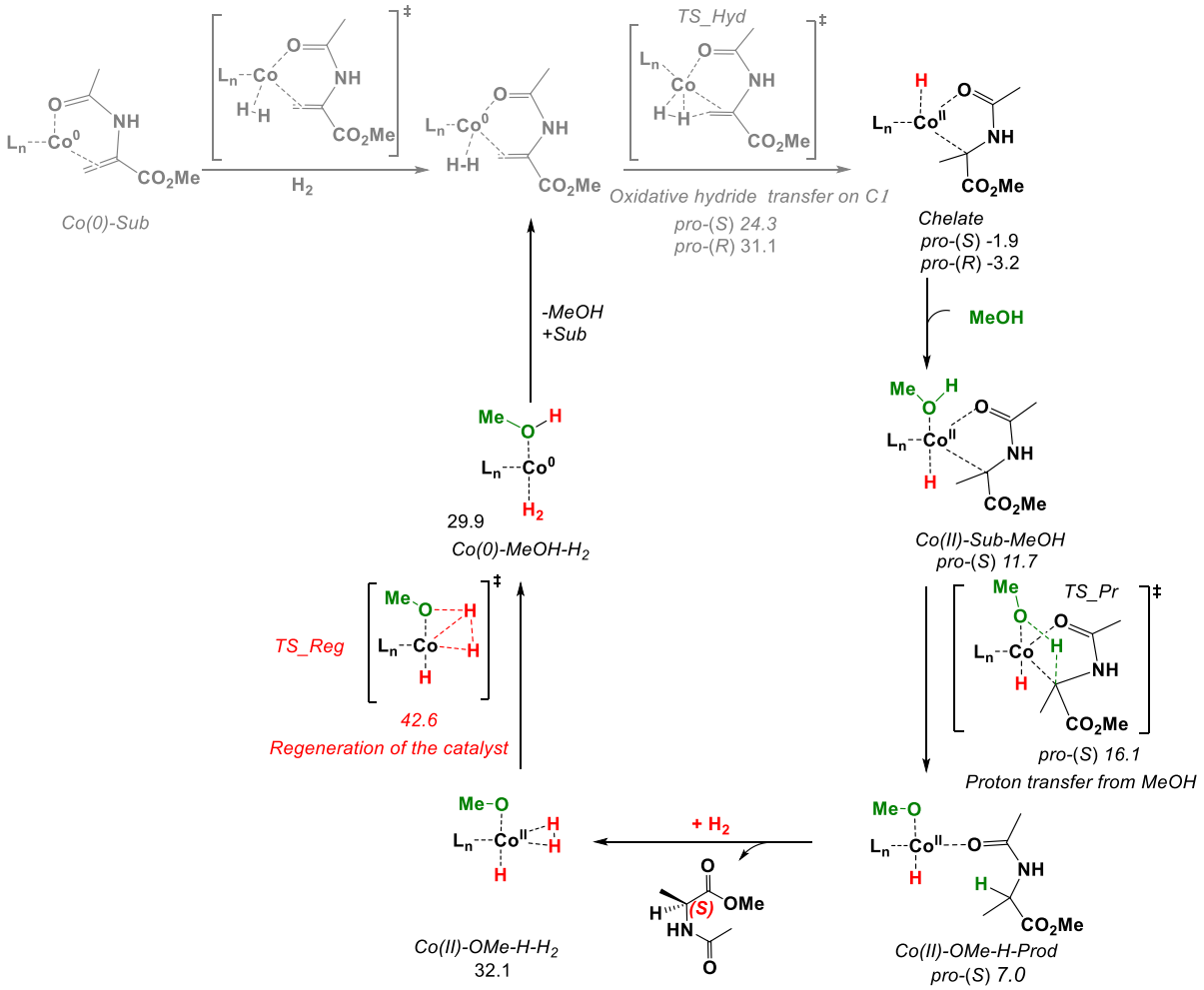

Figure S13. Mechanism and computed free energies (kcal/mol, 323 K, relative to Co-Sub) for Co-^{Ph}BPE-catalyzed hydrogenation of methyl 2-acetamidoacrylate via an alternative MeOH mechanism, in which after formation of the chelate intermediate, coordination of MeOH occurs. In the next step, methanol transfers its proton on C2 atom with reasonable barrier of 18.1 kcal/mol via pro-(*S*) TS_Pr (assuming that the (*R*) and (*S*) intermediates are not in equilibrium ,due to the high backwards barrier). In order to regenerate the catalyst, coordination of one more H_2 molecule must occur, followed by proton transfer from H_2 to the methoxy group. The overall barrier is 44.5 kcal/mol, which is not feasible.

4.9 Mechanism A and C for *dehydro*-levetiracetam with one MeOH hydrogen-bonded to the substrate

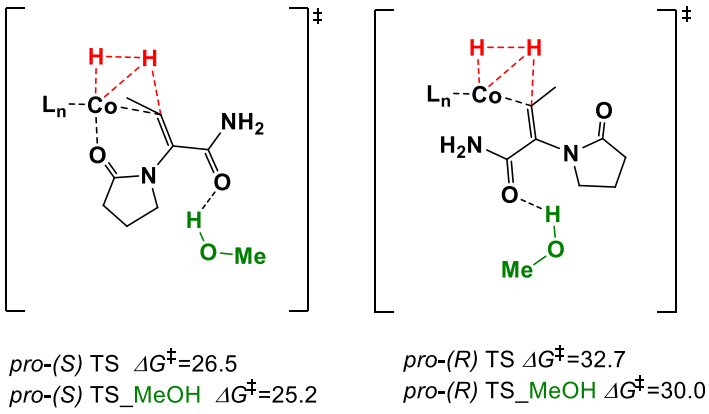

Figure S14a. The optimized pro-(*S*) and -(*R*) TSs for the hydride transfer step and free energies (kcal/mol, 323 K, relative to Co-Sub) for the Co-^{Ph}BPE-catalyzed hydrogenation of *dehydro*-levetiracetam Mechanism **A**, with and without an explicit MeOH-Substrate interaction. The barriers are given relative to the reactant with or without explicit MeOH-Substrate interaction.

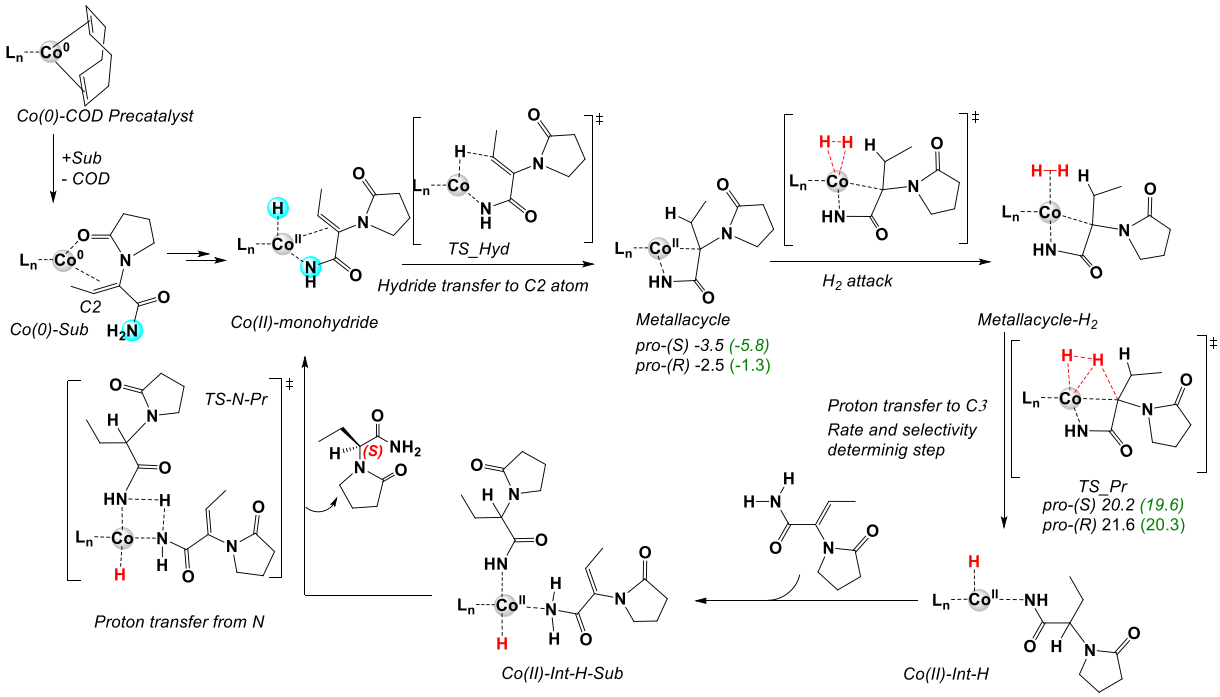

Figure S14b. Proposed non-redox metallacycle mechanism **C** (via a four-membered metallacycle intermediate) and free energies (kcal/mol, 323 K, relative to Co-Sub) for the Co-^{Ph}BPE-catalyzed hydrogenation of *dehydro*-levetiracetam, with computed energies in presence of explicit solvent given in green.

4.10 The computed barriers and enantioselectivities for *dehydro*-levetiracetam and methyl 2-acetamidoacrylate

Table S1. The overall barriers for the Co-^{Ph}BPE-catalyzed hydrogenation of *dehydro*-levetiracetam, without (left) and with (right) explicit MeOH-Substrate interactions, via Mechanism **A** (Figure S2) and **C** (Figure 2 and Figure S4).

Rate-limiting TS	4-mem. metallacycle	4-mem. metallacycle (MeOH)
Pro-(*S*) (Proton transfer to C3)	23.7	25.4
Pro-(*R*) (Proton transfer to C3)	25.1	26.1
TS	5-mem. metallacycle	5-mem. metallacycle (MeOH)
Pro-(*S*) (Hydride transfer to C3)	23.8	**22.8**
Pro-(*R*) (Proton transfer to C2)	24.0	24.1
TS	Redox mechanism	Redox mechanism (MeOH)
Pro-(*S*) (Hydride transfer to C2)	26.5	25.2
Pro-(*R*) (Hydride transfer to C2)	32.7	30.0
e.e.	43.3 % (*S*)	76.6 % (*S*)

Table S2.The overall barriers for the Co-^{Ph}BPE-catalyzed hydrogenation of methyl 2-acetamidoacrylate, without (left) and with (right) explicit MeOH-Substrate interactions, via Mechanisms **A** (Figure 4) and **C** (Figure S8).

Rate-limiting TS	Mechanism A	Mechanism A (MeOH)
Pro-(*S*) (Hydride transfer to C1)	24.3	22.9
Pro-(*R*) (Hydride transfer to C1)	31.1	24.0
TS	Mechanism C (6m)	Mechanism C (6m) (MeOH)
Pro-(*S*) (Proton transfer to C1)	24.0	**20.9**
Pro-(*R*) (Proton transfer to C1)	28.3	23.4
e.e.	99.8 % (*S*)	94.7 % (*S*)

4.11 Proposed mechanism I for the formation of the active Co(II)-monohydride species via an imine intermediate, for methyl 2-acetamidoacrylate substrate

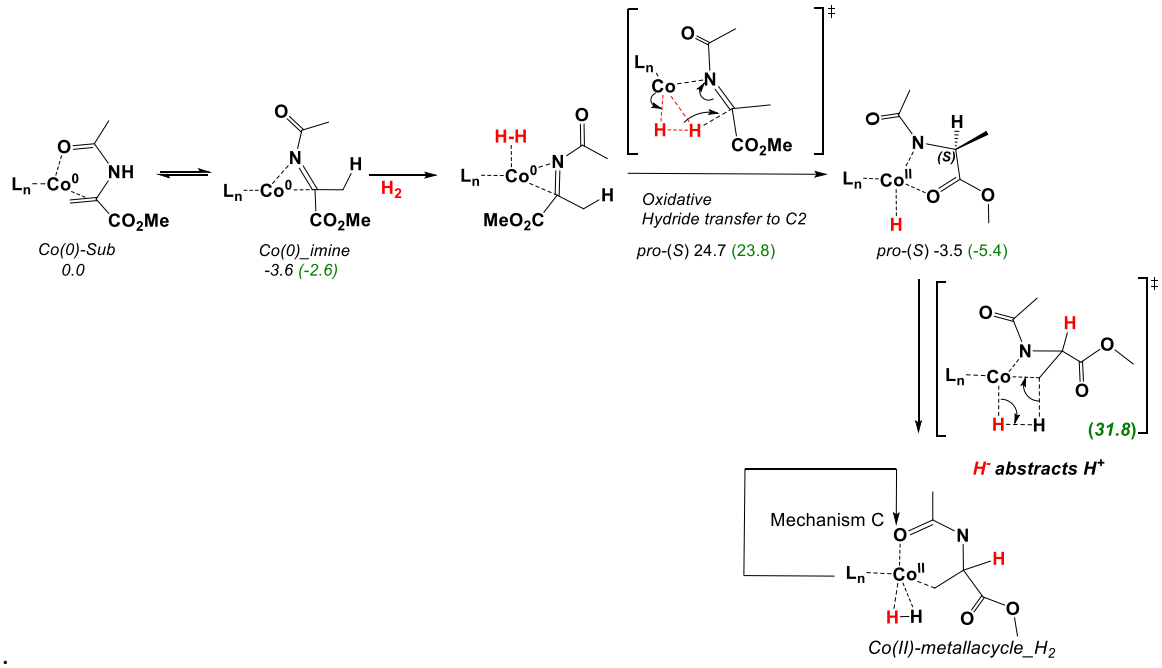

Figure S15. An investigated mechanism for the formation of the active catalyst via imine intermediate. In the next step H_2 binds, followed by hydride transfer to C2 atom. After formation of hydrogenate Co (II) intermediate, a hydride may abstract a proton of the methyl group. This mechanism is excluded due to very high barrier of 37.2 kcal/mol. Energies in parenthesis with green colour are from computational models including an explicit solvent molecule hydrogen-bonded to the substrate

4.12 Proposed mechanism for the formation of the active Co(II)-monohydride species from $CoCl_2$ for methyl 2-acetamidoacrylate substrate

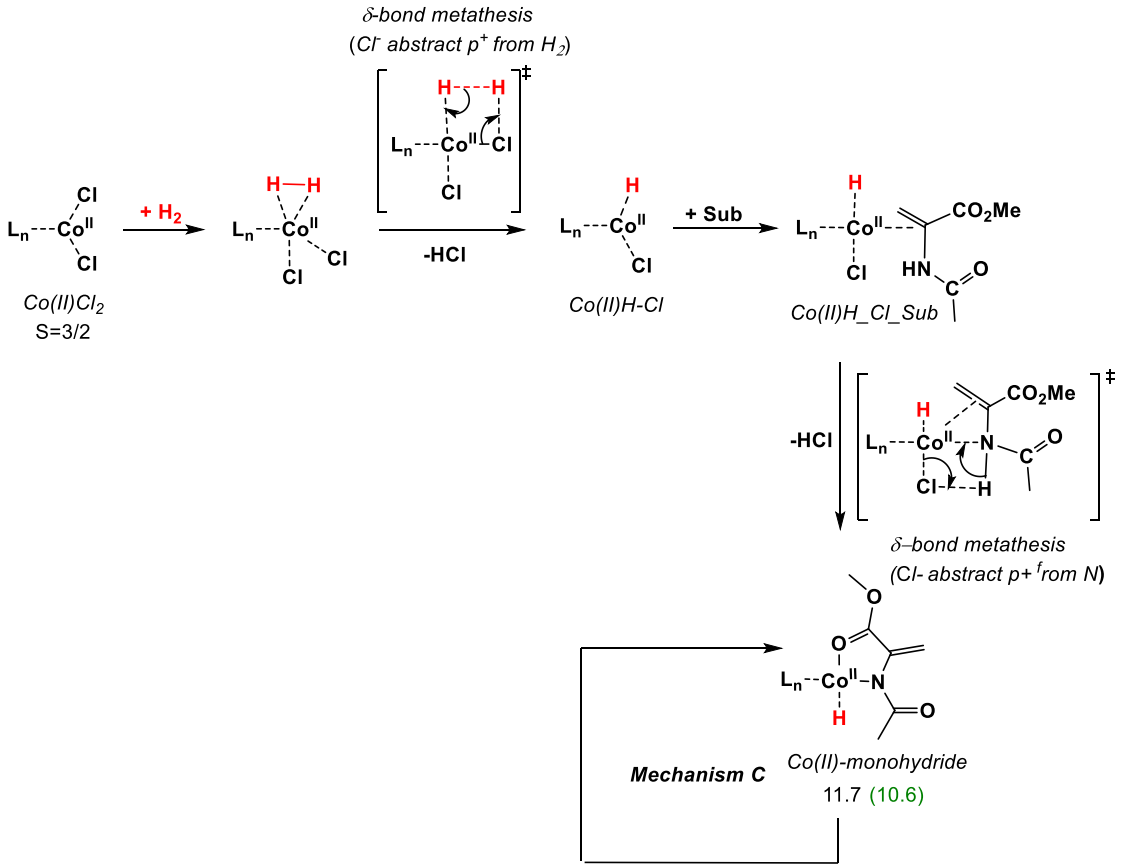

Figure S16. A possible mechanism for the formation of the active catalyst via two σ-bond metathesis steps starting from $CoCl_2$ (S = 3/2). First, the H_2 binds, after which chloride abstracts a proton from H_2. In the next step, HCl is liberated and the Co(II)H-Cl intermediate is formed. Then, the substrate binds and the other chloride abstracts a proton from substrate nitrogen. In this manner, one more molecule of HCl is liberated and the active Co(II)-monohydride is formed. [This mechanism is still ongoing work].

5 Selected coordinates

Methyl 2-acetamidoacrylate (MAA)

Redox Co(0)-Co(II) mechanism **A** with the explicit Solvent-MAA interaction

Pro-(*S*) TS_Hyd with the explicit Solvent-Substrate interaction

G298K=-2776.537463
Img. Freq.=-1222.9488

C	-4.296943000	-2.232616000	-0.210480000
C	-4.081843000	-0.980855000	-0.799998000
C	-4.081590000	-0.902448000	-2.199316000
C	-4.277024000	-2.035295000	-2.984874000
C	-4.478098000	-3.277991000	-2.383752000
C	-4.491383000	-3.369496000	-0.993034000
C	-3.791976000	0.260916000	0.011666000
C	-4.573238000	0.427810000	1.336409000
C	-3.830369000	-0.238279000	2.525074000
C	-2.331003000	-0.467470000	2.193674000
C	-1.284553000	-0.037217000	3.195365000
C	-0.012580000	-0.630541000	3.141764000
C	1.027617000	-0.182930000	3.951061000
C	0.819555000	0.867784000	4.844952000
C	-0.442554000	1.453902000	4.923308000
C	-1.482017000	1.006503000	4.107513000
P	-1.976129000	0.305576000	0.502208000
C	-1.758128000	2.121776000	0.887661000
C	-0.286493000	2.454000000	1.170179000
P	0.868047000	1.628085000	-0.046949000
Co	-0.191339000	-0.093070000	-1.021996000
C	0.419128000	-2.099827000	-1.040654000
N	1.746315000	-2.215390000	-1.587280000
C	2.319478000	-1.224102000	-2.284342000
C	3.708101000	-1.471942000	-2.817501000
C	2.476509000	1.755101000	0.951399000
C	2.882558000	3.227029000	0.746033000
C	2.722513000	3.573632000	-0.744967000
C	1.393776000	2.979544000	-1.282933000
C	0.272898000	3.948680000	-1.563114000
C	-0.653308000	3.664340000	-2.577187000
C	-1.739940000	4.502577000	-2.817401000
C	-1.921557000	5.653297000	-2.050777000
C	-0.999098000	5.959929000	-1.051077000
C	0.085303000	5.117360000	-0.811823000
C	3.528343000	0.710527000	0.621484000
C	4.807835000	1.036417000	0.154752000
C	5.778229000	0.051292000	-0.036277000
C	5.487298000	-1.282676000	0.234978000
C	4.211513000	-1.624037000	0.682765000
C	3.245382000	-0.640698000	0.867956000
C	-0.678514000	-1.829683000	-1.964869000
C	0.227358000	-2.834652000	0.185479000
O	1.130208000	-3.276988000	0.910750000
O	-1.072284000	-3.059331000	0.503310000
C	-1.313456000	-3.947021000	1.608191000
O	1.736184000	-0.143621000	-2.485795000
O	3.059931000	-4.601987000	-0.472209000
H	-0.139132000	3.533637000	1.184332000
H	0.000918000	2.075178000	2.151176000
H	-2.386568000	2.434426000	1.724813000
H	-2.097122000	2.656174000	-0.004074000
H	-5.587768000	0.032370000	1.237079000
H	-4.671975000	1.498272000	1.531156000
H	-3.954286000	0.374641000	3.417665000
H	-4.282380000	-1.203579000	2.764877000
H	-3.913079000	0.057694000	-2.675500000
H	-4.269475000	-1.948363000	-4.065747000
H	-4.626580000	-4.162883000	-2.992058000
H	-4.648096000	-4.329039000	-0.512807000
H	-4.305113000	-2.330879000	0.867305000
H	0.174295000	-1.436350000	2.442923000
H	2.003074000	-0.650165000	3.874548000
H	1.628941000	1.222238000	5.472653000
H	-0.620215000	2.269681000	5.615261000
H	-2.444658000	1.498257000	4.173551000
H	3.544932000	3.131501000	-1.311052000
H	2.773536000	4.652163000	-0.908272000
H	2.221221000	3.858442000	1.345749000
H	3.897103000	3.424600000	1.102027000
H	-0.518823000	2.772288000	-3.176890000
H	-2.442109000	4.258384000	-3.607079000
H	-2.765745000	6.307791000	-2.235885000
H	-1.122362000	6.856938000	-0.454238000
H	0.789220000	5.377509000	-0.029496000
H	2.253119000	-0.931770000	1.188230000
H	3.962549000	-2.660414000	0.868270000
H	6.238753000	-2.049870000	0.085627000
H	6.761654000	0.333264000	-0.396431000
H	5.071619000	2.065435000	-0.051069000
H	2.178256000	1.586167000	1.989272000
H	1.586313000	2.403687000	-2.187928000
H	-2.181374000	-1.526267000	1.993633000
H	-3.960238000	1.129479000	-0.629010000
H	-1.058487000	-0.333806000	-2.238574000
H	-0.930913000	0.812496000	-2.021371000
H	2.293027000	-3.047980000	-1.376165000
H	4.366482000	-0.699050000	-2.417530000
H	4.100995000	-2.449713000	-2.538198000
H	3.694877000	-1.381755000	-3.905965000
H	-1.645406000	-2.238135000	-1.698296000
H	-0.428148000	-1.966531000	-3.014682000
H	-0.937406000	-3.528842000	2.543339000
H	-2.394622000	-4.058621000	1.653809000
H	-0.840359000	-4.914572000	1.434443000
H	2.448304000	-4.221036000	0.188592000
C	2.517870000	-5.850171000	-0.906495000
H	1.519290000	-5.732130000	-1.345349000
H	3.185319000	-6.252579000	-1.669971000
H	2.455896000	-6.572058000	-0.083923000

Pro-(*R*) TS_Hyd with the explicit Solvent-Substrate interaction

G298K=-2776.532847
Img. Freq.=-1171.8315

C	-4.633704000	-0.039049000	-0.254705000
C	-4.022058000	1.216081000	-0.135095000
C	-4.119631000	2.100769000	-1.217147000
C	-4.800236000	1.746807000	-2.379945000
C	-5.402324000	0.493462000	-2.484738000
C	-5.317046000	-0.396125000	-1.415436000
C	-3.209977000	1.622568000	1.074018000
C	-3.790049000	1.280455000	2.466135000
C	-3.385930000	-0.146578000	2.893843000
C	-2.002674000	-0.538119000	2.299242000
C	-0.881528000	-0.818023000	3.271522000
C	0.110240000	-1.749321000	2.932142000
C	1.210330000	-1.957625000	3.761944000
C	1.342781000	-1.239770000	4.950118000
C	0.353268000	-0.323940000	5.307291000
C	-0.748281000	-0.118601000	4.478411000
P	-1.514125000	0.808021000	1.047868000
C	-0.503129000	2.054206000	1.997102000
C	0.981311000	1.669042000	2.018862000
P	1.590958000	0.969703000	0.384625000
Co	-0.207507000	0.509385000	-0.862496000
C	-0.778611000	-1.286885000	-1.706327000
N	-1.544941000	-2.188398000	-0.895111000
C	-2.601091000	-2.905234000	-1.372015000
C	-3.251728000	-3.828618000	-0.357658000
C	3.076832000	0.001237000	1.037398000
C	4.023843000	1.108036000	1.567939000
C	3.917874000	2.403963000	0.710208000
C	2.750614000	2.287449000	-0.299286000
C	2.054331000	3.556423000	-0.716402000
C	1.694553000	3.734393000	-2.058766000
C	0.985193000	4.858785000	-2.474182000
C	0.612180000	5.832214000	-1.548183000
C	0.965176000	5.671143000	-0.208770000
C	1.681377000	4.547676000	0.200849000
C	3.694540000	-0.946409000	0.034276000
C	4.742795000	-0.571675000	-0.817858000
C	5.339367000	-1.501316000	-1.669791000
C	4.896564000	-2.823238000	-1.689994000
C	3.838482000	-3.200785000	-0.864438000
C	3.245579000	-2.271917000	-0.014739000
C	-1.467146000	-0.159758000	-2.312082000
C	0.378215000	-1.880217000	-2.364284000
O	0.835449000	-3.000742000	-2.141268000
O	0.956430000	-1.048704000	-3.265302000
C	2.202396000	-1.486897000	-3.838362000
O	-3.048035000	-2.786348000	-2.508568000
O	0.465705000	-3.925110000	0.427500000
C	0.146521000	-5.312208000	0.482632000
H	1.591956000	2.522625000	2.314512000
H	1.152367000	0.887467000	2.760202000
H	-0.874551000	2.206777000	3.012188000
H	-0.638523000	2.988513000	1.445860000
H	-4.876676000	1.402449000	2.476525000
H	-3.383332000	1.999629000	3.182716000
H	-3.382083000	-0.227484000	3.982083000
H	-4.127592000	-0.867160000	2.545412000
H	-3.646316000	3.074714000	-1.149693000
H	-4.858007000	2.449210000	-3.204033000
H	-5.927321000	0.211743000	-3.390172000
H	-5.767592000	-1.378837000	-1.489543000
H	-4.567990000	-0.756534000	0.551987000
H	0.036477000	-2.316614000	2.011398000
H	1.965608000	-2.681139000	3.474812000
H	2.201396000	-1.396217000	5.592921000
H	0.439579000	0.236060000	6.231773000
H	-1.498991000	0.605963000	4.771962000
H	4.844707000	2.593080000	0.163000000
H	3.772892000	3.264213000	1.364616000
H	3.742963000	1.332574000	2.598472000
H	5.051037000	0.739062000	1.601479000
H	1.967790000	2.975207000	-2.783918000
H	0.721311000	4.972104000	-3.519849000
H	0.057966000	6.707808000	-1.866508000
H	0.685332000	6.422646000	0.521155000

H	1.946124000	4.450515000	1.246442000
H	2.424588000	-2.585393000	0.618413000
H	3.466420000	-4.218511000	-0.883368000
H	5.363199000	-3.546178000	-2.349465000
H	6.154514000	-1.190721000	-2.314020000
H	5.121056000	0.443314000	-0.807102000
H	2.698908000	-0.596013000	1.868490000
H	3.125964000	1.801755000	-1.205151000
H	-2.129612000	-1.422580000	1.674547000
H	-3.031724000	2.697936000	1.007185000
H	-1.060511000	1.290897000	-1.828631000
H	-0.341628000	1.996372000	-1.176016000
H	-1.105870000	-2.531110000	-0.052548000
H	-3.482964000	-4.778671000	-0.840398000
H	-2.636594000	-4.006429000	0.525538000
H	-4.194734000	-3.376482000	-0.038350000
H	-2.531073000	-0.102287000	-2.122328000
H	-1.198320000	0.071998000	-3.338419000
H	2.081626000	-2.449727000	-4.336762000
H	2.475261000	-0.719259000	-4.559501000
H	2.963755000	-1.571595000	-3.064437000
H	0.647910000	-3.683376000	-0.504097000
H	-0.702364000	-5.563506000	-0.164936000
H	1.001330000	-5.937159000	0.197105000
H	-0.124580000	-5.549276000	1.512964000

Non-redox metallacycle mechanism **C** with the explicit Solvent-MAA interaction

Pro-(*S*) TS_Pr (C1) with the explicit Solvent-Substrate interaction

G298K= -2776.537452
Img. Freq.=-1012.293

P	1.477355000	0.451198000	1.446652000
P	1.169279000	-1.030208000	-1.345591000
C	2.621271000	-1.449463000	-0.245254000
C	2.997434000	-0.278777000	0.678667000
H	3.481590000	-1.768158000	-0.837551000
H	2.298331000	-2.307512000	0.349543000
H	3.703763000	-0.597878000	1.448614000
H	3.464920000	0.528125000	0.108648000
C	0.793390000	-2.715090000	-2.136162000
C	1.956267000	-0.341796000	-2.930333000
C	2.037619000	2.038224000	2.296027000
C	1.164539000	-0.476727000	3.051033000
C	1.681564000	1.823606000	3.787815000
C	1.453476000	3.263065000	1.635801000
H	0.631977000	2.077171000	3.963057000
H	2.282538000	2.483815000	4.417551000
C	1.912728000	0.343860000	4.117920000
C	1.446441000	-1.956106000	2.947882000
H	2.985946000	0.133279000	4.089261000
H	1.559074000	0.089216000	5.120685000
C	2.269644000	4.129552000	0.903927000
C	1.727732000	5.218792000	0.220286000
C	0.355615000	5.457656000	0.258092000
C	-0.470646000	4.600030000	0.986848000
C	0.074029000	3.515273000	1.666671000
H	3.336449000	3.940717000	0.852151000
H	2.379230000	5.876670000	-0.344140000
H	-0.067694000	6.300878000	-0.275636000
H	-1.541557000	4.768164000	1.014858000
H	-0.586144000	2.840211000	2.200109000
C	0.453940000	-2.800707000	2.428415000
C	0.690991000	-4.162025000	2.262536000
C	1.929160000	-4.708104000	2.603450000
C	2.922864000	-3.878246000	3.118959000
C	2.682694000	-2.514776000	3.293304000
H	-0.490048000	-2.364759000	2.122571000
H	-0.090806000	-4.793795000	1.858247000
H	2.116202000	-5.767597000	2.469870000
H	3.888772000	-4.290153000	3.389685000
H	3.470810000	-1.891918000	3.698170000
C	2.258505000	-1.578772000	-3.794287000
C	3.077210000	0.633236000	-2.670199000
H	2.430601000	-1.292326000	-4.835686000
H	3.162423000	-2.086031000	-3.444521000
C	1.060992000	-2.521026000	-3.648302000
C	-0.563850000	-3.278495000	-1.791907000
H	1.235732000	-3.488235000	-4.126541000
H	0.185326000	-2.076387000	-4.130679000
C	2.783648000	1.993351000	-2.496558000
C	3.776119000	2.909499000	-2.160198000
C	5.095090000	2.485808000	-2.000004000
C	5.408380000	1.141944000	-2.196910000
C	4.411131000	0.226634000	-2.531544000
H	1.762693000	2.335280000	-2.618219000
H	3.516155000	3.951889000	-2.019289000
H	5.869876000	3.195724000	-1.734165000
H	6.432042000	0.801101000	-2.089054000
H	4.682774000	-0.811226000	-2.677207000
C	-0.670114000	-4.438668000	-1.018073000
C	-1.916444000	-4.976069000	-0.695848000
C	-3.081954000	-4.357395000	-1.143086000
C	-2.990432000	-3.196183000	-1.911208000
C	-1.744612000	-2.666830000	-2.233243000
H	0.232013000	-4.924260000	-0.662935000
H	-1.974207000	-5.877038000	-0.095046000
H	-4.052138000	-4.768449000	-0.888786000
H	-3.889955000	-2.696507000	-2.252000000
H	-1.691907000	-1.764480000	-2.830834000
H	1.557691000	-3.390615000	-1.742203000
H	1.131002000	0.203747000	-3.399388000
H	0.088372000	-0.343752000	3.193663000
H	3.126648000	2.064061000	2.199878000
Co	-0.156494000	0.529888000	-0.083333000
C	-2.672158000	-0.612563000	0.827875000
C	-3.319974000	-1.815980000	1.473941000
H	-4.392561000	-1.838773000	1.283851000
H	-2.861869000	-2.726053000	1.081081000
H	-3.138880000	-1.789105000	2.552074000
O	-1.398958000	-0.498430000	1.035643000
C	-2.821501000	1.391698000	-0.432498000
N	-3.434639000	0.198203000	0.156932000
C	-1.682145000	1.085812000	-1.407427000
H	-1.625122000	1.867550000	-2.170573000
H	-1.860934000	0.149268000	-1.932136000
C	-3.991049000	2.095542000	-1.116883000
C	-5.981809000	3.301389000	-0.695229000
H	-6.636300000	2.454028000	-0.904673000
H	-6.380185000	3.898836000	0.121178000
H	-5.854362000	3.909691000	-1.590857000
O	-4.281689000	2.002612000	-2.287873000
O	-4.709250000	2.803644000	-0.228806000
H	-2.463748000	2.066303000	0.359310000
H	0.637845000	1.695530000	-0.696080000
H	-0.284193000	1.632519000	-1.125574000
C	-6.457619000	0.536269000	1.542320000
H	-6.074745000	1.558314000	1.662028000
H	-7.543825000	0.561250000	1.667534000
H	-6.039458000	-0.077352000	2.354224000
H	-5.175451000	0.038302000	0.164957000
O	-6.164531000	0.004277000	0.260637000

Pro-(*R*) TS_Pr (C1) with the explicit Solvent-Substrate interaction

G298K= -2776.534086
Img. Freq.=-1003.0208

P	1.880771000	-0.586130000	1.113207000
P	0.238297000	-0.424938000	-1.637175000
C	1.485197000	-1.792304000	-1.372772000
C	2.599219000	-1.385068000	-0.394459000
H	1.907221000	-2.124730000	-2.323422000
H	0.914445000	-2.628446000	-0.958400000
H	3.215182000	-2.245097000	-0.124520000
H	3.253475000	-0.635000000	-0.845444000
C	-1.041196000	-1.290097000	-2.751789000
C	0.925843000	0.618349000	-3.071593000
C	3.346313000	0.125057000	2.057143000
C	1.514937000	-1.920743000	2.392385000
C	3.158368000	-0.423126000	3.491287000
C	3.485518000	1.622420000	1.946550000
H	2.395150000	0.158666000	4.017456000
H	4.087857000	-0.324792000	4.057379000
C	2.709649000	-1.882475000	3.368016000
C	1.136819000	-3.259995000	1.808622000
H	3.542708000	-2.479216000	2.987010000
H	2.424412000	-2.305855000	4.334765000
C	4.602531000	2.185174000	1.323223000
C	4.733896000	3.568881000	1.199598000
C	3.744393000	4.413155000	1.697944000
C	2.622776000	3.863301000	2.321991000
C	2.496123000	2.483210000	2.443260000
H	5.372188000	1.535270000	0.920978000
H	5.608416000	3.983975000	0.711014000
H	3.843109000	5.488341000	1.601084000
H	1.842681000	4.510132000	2.707667000
H	1.607342000	2.069708000	2.907191000
C	-0.215111000	-3.551151000	1.580277000
C	-0.598971000	-4.773347000	1.033955000
C	0.360618000	-5.723078000	0.685038000
C	1.709064000	-5.439403000	0.894399000
C	2.092334000	-4.221966000	1.455167000
H	-0.956699000	-2.795187000	1.812105000
H	-1.650144000	-4.985195000	0.878581000
H	0.060757000	-6.672526000	0.256458000
H	2.466283000	-6.167924000	0.626777000
H	3.145950000	-4.029637000	1.616559000
C	0.318120000	0.011730000	-4.350352000
C	2.421285000	0.807474000	-3.028963000
H	0.352939000	0.732882000	-5.171525000
H	0.881362000	-0.869669000	-4.669657000
C	-1.115323000	-0.402447000	-4.008230000
C	-2.341109000	-1.633298000	-2.062294000
H	-1.598292000	-0.940033000	-4.828477000
H	-1.709832000	0.495405000	-3.814718000
C	2.962061000	1.901447000	-2.338922000
C	4.338599000	2.062546000	-2.207029000
C	5.210119000	1.131412000	-2.770474000
C	4.688589000	0.049527000	-3.478223000
C	3.309835000	-0.108343000	-3.609110000
H	2.295323000	2.629955000	-1.892090000
H	4.726859000	2.910726000	-1.656755000
H	6.282256000	1.251422000	-2.665037000
H	5.355107000	-0.676453000	-3.930335000
H	2.931876000	-0.959046000	-4.162126000
C	-2.409933000	-2.791002000	-1.274618000
C	-3.572607000	-3.125721000	-0.586744000
C	-4.701035000	-2.310807000	-0.679957000
C	-4.649742000	-1.164874000	-1.468640000
C	-3.483088000	-0.830329000	-2.154337000
H	-1.539060000	-3.431432000	-1.193091000

H	-3.602512000	-4.024004000	0.019371000
H	-5.607127000	-2.566023000	-0.142567000
H	-5.513016000	-0.515115000	-1.541130000
H	-3.473056000	0.078275000	-2.741693000
H	-0.556717000	-2.228852000	-3.039778000
H	0.456093000	1.592985000	-2.906856000
H	0.634763000	-1.511508000	2.894457000
H	4.234399000	-0.347556000	1.626489000
Co	0.158419000	0.734411000	0.493904000
C	-2.347043000	0.072712000	1.793372000
C	-3.017017000	-0.691618000	2.915330000
H	-4.007503000	-0.291537000	3.129697000
H	-3.111356000	-1.741459000	2.621535000
H	-2.397078000	-0.657332000	3.814748000
O	-1.126593000	-0.287775000	1.549060000
C	-2.493034000	1.676673000	0.031181000
N	-3.053633000	0.975288000	1.184757000
C	-1.144752000	2.373328000	0.265991000
H	-1.018653000	3.156675000	-0.489300000
H	-1.138638000	2.869640000	1.241719000
C	-3.585825000	2.665161000	-0.371004000
C	-4.816307000	4.558163000	0.343132000
H	-5.705369000	4.007689000	0.654884000
H	-4.636543000	5.398136000	1.010219000
H	-4.923260000	4.900637000	-0.686225000
O	-4.320727000	2.527340000	-1.325703000
O	-3.667774000	3.696612000	0.483303000
H	-2.405944000	0.995230000	-0.815696000
H	1.237264000	1.689809000	-0.018756000
H	0.304851000	2.138319000	-0.051270000
C	-6.440737000	0.886140000	1.077120000
H	-6.215291000	-0.189326000	1.090213000
H	-7.480450000	1.017576000	1.390285000
H	-6.348580000	1.235498000	0.039572000
H	-4.669272000	1.416433000	1.711906000
O	-5.609908000	1.621508000	1.961681000

Dehydro-levetiracetam

Non-redox 4-membered metallacycle mechanism **C** with the explicit Solvent-Dehydro-levetiracetam interaction

Pro-(*S*) TS_Pr (C3) with the explicit Solvent-Substrate interaction

G298K=-2834.076875
Img. Freq.=-1256.251 cm-1

C	-4.027730000	-0.982694000	-1.190271000
C	-2.987984000	-0.768699000	-2.100703000
C	-2.927589000	0.462985000	-2.763260000
C	-3.883595000	1.446640000	-2.528802000
C	-4.914559000	1.222186000	-1.616911000
C	-4.981319000	0.003464000	-0.944706000
C	-1.936203000	-1.832053000	-2.302734000
C	-1.580175000	-2.168338000	-3.772776000
C	-0.169919000	-2.768841000	-3.806475000
C	0.728534000	-1.815782000	-2.998708000
C	2.141160000	-2.244805000	-2.699325000
C	3.155212000	-1.278438000	-2.634913000
C	4.464149000	-1.632057000	-2.316563000
C	4.786759000	-2.961355000	-2.046688000
C	3.790162000	-3.933525000	-2.115242000
C	2.482683000	-3.579460000	-2.443921000
P	-0.290276000	-1.414009000	-1.463759000
C	-0.038488000	-2.849352000	-0.306096000
C	1.072656000	-2.564094000	0.714890000
P	0.828483000	-0.888605000	1.493168000
Co	0.088218000	0.457466000	-0.317451000
N	-1.661049000	1.093515000	0.272913000
C	-1.100559000	2.048514000	1.007263000
O	-1.455766000	2.522898000	2.111063000
C	2.369332000	-0.680920000	2.583323000
C	1.803825000	-0.432768000	3.994824000
C	0.603584000	-1.363151000	4.182060000
C	-0.329837000	-1.147118000	2.975152000
C	-1.416704000	-2.171999000	2.760142000
C	-2.691765000	-1.757183000	2.352707000
C	-3.694271000	-2.685352000	2.078756000
C	-3.445778000	-4.050961000	2.208466000
C	-2.189619000	-4.476236000	2.639690000
C	-1.189664000	-3.546857000	2.918683000
C	3.362818000	0.337004000	2.060180000
C	3.881475000	0.199574000	0.764588000
C	4.778957000	1.126505000	0.245703000
C	5.189491000	2.214427000	1.017085000
C	4.698910000	2.353115000	2.312228000
C	3.796059000	1.422459000	2.828390000
C	0.208326000	2.477259000	0.310902000
C	1.224310000	3.125987000	1.254853000
H	1.238234000	2.525693000	2.165671000
N	-0.079355000	3.261822000	-0.886643000
C	0.887727000	3.589003000	-1.787665000
C	0.273342000	4.502836000	-2.837528000
C	-1.237184000	4.322726000	-2.642321000
C	-1.368360000	3.914117000	-1.166345000
O	2.057682000	3.218323000	-1.736566000
C	0.903222000	4.587045000	1.586291000
H	0.161125000	-3.766830000	-0.862624000
H	-0.994388000	-2.981267000	0.206183000
H	1.125239000	-3.355247000	1.464793000
H	2.044385000	-2.524291000	0.215145000
H	1.467189000	0.605468000	4.086357000
H	2.570083000	-0.593806000	4.757576000
H	0.950639000	-2.399581000	4.222952000
H	0.072846000	-1.162405000	5.116845000
H	3.426752000	1.561380000	3.836346000
H	5.012137000	3.190413000	2.926115000
H	5.883536000	2.942245000	0.612326000
H	5.150923000	1.005645000	-0.764973000
H	3.572291000	-0.632825000	0.144239000
H	-2.916295000	-0.700489000	2.269565000
H	-4.673074000	-2.336942000	1.768192000
H	-4.223335000	-4.773911000	1.989576000
H	-1.985796000	-5.534289000	2.761345000
H	-0.224622000	-3.904538000	3.255254000
H	0.201607000	-2.878317000	-4.828902000
H	-0.183035000	-3.767153000	-3.359096000
H	-2.325495000	-2.847934000	-4.192779000
H	-1.596625000	-1.259645000	-4.380234000
H	2.911293000	-0.240092000	-2.830013000
H	5.233331000	-0.869413000	-2.280005000
H	5.804119000	-3.236920000	-1.793977000
H	4.029550000	-4.972349000	-1.917460000
H	1.729131000	-4.354917000	-2.501523000
H	-4.080822000	-1.925581000	-0.657935000
H	-5.772343000	-0.179448000	-0.226113000
H	-5.653782000	1.991758000	-1.427409000
H	-3.818800000	2.394358000	-3.051340000
H	-2.116495000	0.668190000	-3.453157000
H	-2.271210000	-2.749443000	-1.812201000
H	0.766959000	-0.859185000	-3.529259000
H	-0.802468000	-0.165291000	3.079241000
H	2.854477000	-1.663817000	2.579890000
H	2.220816000	3.058647000	0.819176000
H	-2.508895000	0.682905000	0.646282000
H	-1.498044000	4.779678000	-0.507251000
H	-2.185182000	3.214892000	-0.999281000
H	-1.595204000	3.506862000	-3.274895000
H	-1.818801000	5.214570000	-2.875408000
H	0.598382000	5.526197000	-2.620015000
H	0.637894000	4.242888000	-3.831655000
H	1.490234000	0.555681000	-0.894936000
H	1.187916000	1.509025000	-0.342467000
H	1.638369000	4.986112000	2.290922000
H	0.933346000	5.210143000	0.687875000
H	-0.088452000	4.672024000	2.032172000
C	-4.763405000	2.287179000	1.917129000
H	-4.887866000	3.243720000	2.443086000
H	-4.427368000	2.493434000	0.893777000
H	-5.739992000	1.801234000	1.856964000
O	-3.874969000	1.412333000	2.602440000
H	-2.980047000	1.818679000	2.549599000

Pro-(*R*) TS_Pr (C3) with the explicit Solvent-Substrate interaction

G298K=-2834.075684
Img. Freq.=-1207.331 cm-1

C	-4.782618000	-0.162206000	0.741285000
C	-3.887412000	0.509301000	1.581109000
C	-3.521709000	-0.101838000	2.786708000
C	-4.040121000	-1.342275000	3.145384000
C	-4.931260000	-2.003206000	2.299533000
C	-5.299511000	-1.408494000	1.094062000
C	-3.280969000	1.818006000	1.140323000
C	-3.240029000	2.956872000	2.185878000
C	-2.189593000	3.976951000	1.727820000
C	-0.901837000	3.183553000	1.446017000
C	0.238227000	3.872038000	0.738725000
C	1.552759000	3.447051000	0.983188000
C	2.620737000	3.992466000	0.274504000
C	2.400170000	4.979879000	-0.685294000
C	1.100325000	5.425190000	-0.920998000
C	0.030220000	4.877114000	-0.214961000
P	-1.494038000	1.636591000	0.540739000
C	-1.613849000	2.104715000	-1.251836000
C	-0.328962000	1.756993000	-2.011188000
P	0.312727000	0.046714000	-1.608224000
Co	-0.337101000	-0.256481000	0.705314000
N	-1.644853000	-1.648992000	0.597532000
C	-0.846534000	-2.690000000	0.789334000
O	-1.052458000	-3.900706000	0.611155000
C	1.939933000	0.096208000	-2.608762000
C	1.796275000	-0.981492000	-3.705543000
C	0.328523000	-1.029118000	-4.131011000
C	-0.511874000	-1.130302000	-2.846362000
C	-2.005689000	-0.999078000	-3.012125000
C	-2.854207000	-1.917517000	-2.380526000
C	-4.238661000	-1.808776000	-2.483566000
C	-4.807161000	-0.779007000	-3.232182000
C	-3.975219000	0.125531000	-3.890643000
C	-2.589739000	0.011759000	-3.787320000
C	3.237731000	0.066509000	-1.822609000
C	3.315702000	0.603155000	-0.533445000
C	4.527412000	0.673434000	0.149411000
C	5.696538000	0.208231000	-0.447762000
C	5.635950000	-0.338473000	-1.729827000
C	4.419784000	-0.411740000	-2.407998000
C	0.472480000	-2.117989000	1.391586000
C	0.371799000	-2.256383000	2.933949000

H	1.119158000	-1.621127000	3.408067000
N	1.678400000	-2.703612000	0.839843000
C	2.921245000	-2.349443000	1.255436000
C	3.950033000	-3.005434000	0.358179000
C	3.143412000	-4.018510000	-0.461318000
C	1.717959000	-3.449238000	-0.430233000
O	3.173854000	-1.584490000	2.190880000
C	0.529651000	-3.695038000	3.436812000
H	-1.858537000	3.163954000	-1.358543000
H	-2.456460000	1.533784000	-1.647619000
H	-0.465892000	1.879515000	-3.087646000
H	0.476544000	2.434111000	-1.712363000
H	2.102570000	-1.956232000	-3.311569000
H	2.446470000	-0.762457000	-4.555670000
H	0.076697000	-0.119557000	-4.684968000
H	0.122777000	-1.875852000	-4.791944000
H	4.401313000	-0.836950000	-3.403790000
H	6.535952000	-0.714104000	-2.204166000
H	6.641228000	0.258744000	0.081647000
H	4.537968000	1.078116000	1.153270000
H	2.418382000	0.959536000	-0.047401000
H	-2.420863000	-2.719859000	-1.794689000
H	-4.871898000	-2.526567000	-1.975026000
H	-5.884587000	-0.688113000	-3.309176000
H	-4.403470000	0.922587000	-4.488158000
H	-1.965725000	0.723541000	-4.313369000
H	-2.012249000	4.748410000	2.481978000
H	-2.543317000	4.482395000	0.824195000
H	-4.230471000	3.405964000	2.292593000
H	-2.956363000	2.563466000	3.166016000
H	1.744703000	2.673849000	1.719637000
H	3.625995000	3.636179000	0.467938000
H	3.231575000	5.401553000	-1.238697000
H	0.915420000	6.199851000	-1.656946000
H	-0.970683000	5.237419000	-0.417946000
H	-5.061092000	0.281575000	-0.208669000
H	-5.985537000	-1.914190000	0.423914000
H	-5.329344000	-2.973113000	2.575079000
H	-3.734479000	-1.802012000	4.078530000
H	-2.802110000	0.378842000	3.439500000
H	-3.833661000	2.180345000	0.269129000
H	-0.531141000	2.791463000	2.397776000
H	-0.321396000	-2.110126000	-2.398400000
H	1.899773000	1.071456000	-3.107953000
H	-0.609428000	-1.860892000	3.210211000
H	-2.595292000	-1.820817000	0.298977000
H	1.543407000	-2.756132000	-1.259149000
H	0.940598000	-4.206664000	-0.442828000
H	3.156129000	-4.996178000	0.025686000
H	3.510699000	-4.139736000	-1.480634000
H	4.379458000	-2.217400000	-0.265673000
H	4.757608000	-3.434800000	0.952117000
H	0.854402000	0.469789000	1.322764000
H	0.927417000	-0.649016000	1.434839000
H	0.406248000	-3.732126000	4.522740000
H	-0.207258000	-4.354893000	2.976714000
H	1.523563000	-4.081619000	3.197451000
C	3.851119000	1.103001000	4.021117000
H	3.801283000	2.093658000	4.477524000
H	3.748288000	0.352388000	4.814925000
H	4.843063000	0.986783000	3.563887000
O	2.804553000	1.014186000	3.061073000
H	2.835363000	0.118584000	2.679097000

Non-redox 5-membered metallacycle mechanism **C** with the explicit Solvent-Dehydro-levetiracetam interaction

Pro-(*S*) TS_Hyd (C3) with the explicit Solvent-substrate interaction

G298K=-2832.892788
Img. Freq.=-452.8544

C	-4.769313000	-0.696559000	-0.927679000
C	-3.845862000	-0.507774000	-1.964135000
C	-3.989211000	0.621979000	-2.778415000
C	-5.023583000	1.531107000	-2.565183000
C	-5.933981000	1.332759000	-1.529352000
C	-5.800586000	0.213588000	-0.708420000
C	-2.752995000	-1.527521000	-2.177809000
C	-2.241125000	-1.689966000	-3.623286000
C	-1.003113000	-2.583800000	-3.566088000
C	-0.053395000	-1.969303000	-2.522691000
C	1.079605000	-2.832700000	-2.027704000
C	2.285279000	-2.228582000	-1.648968000
C	3.333786000	-2.979906000	-1.126844000
C	3.196982000	-4.358753000	-0.970740000
C	2.005652000	-4.975587000	-1.351028000
C	0.957975000	-4.220558000	-1.877326000
P	-1.175222000	-1.299211000	-1.148472000
C	-1.293450000	-2.643690000	0.142718000
C	-0.077609000	-2.630546000	1.084425000
P	0.471258000	-0.890002000	1.448229000
Co	-0.238042000	0.493819000	-0.142344000
N	1.301492000	1.152772000	-1.771751000
C	1.214163000	2.398789000	-1.359377000
O	1.976168000	3.390069000	-1.533241000
C	2.124468000	-1.094141000	2.321513000
C	1.963333000	-0.262024000	3.616997000
C	0.567856000	-0.565910000	4.172118000
C	-0.424667000	-0.323727000	3.020597000
C	-1.821633000	-0.875726000	3.128895000
C	-2.871897000	-0.180869000	2.513939000
C	-4.170737000	-0.680098000	2.529520000
C	-4.446020000	-1.894919000	3.157125000
C	-3.411081000	-2.596007000	3.774057000
C	-2.111544000	-2.089528000	3.763458000
C	3.401269000	-0.815840000	1.561944000
C	4.538606000	-1.576929000	1.860779000
C	5.746811000	-1.345072000	1.206382000
C	5.830067000	-0.355564000	0.226271000
C	4.704127000	0.410120000	-0.078675000
C	3.504613000	0.190326000	0.597814000
O	1.555877000	2.826669000	1.971654000
C	0.877133000	3.739644000	1.515053000
N	0.008941000	3.644800000	0.461749000
C	-0.483332000	4.965734000	0.031695000
C	-0.334394000	5.815442000	1.301492000
C	0.865777000	5.176824000	2.011324000
C	-0.020154000	2.555579000	-0.468057000
C	-1.262333000	2.090760000	-0.975827000
H	0.511111000	1.461068000	0.716314000
H	-1.409060000	-3.620654000	-0.331921000
H	-2.208558000	-2.433520000	0.703560000
H	-0.295576000	-3.164309000	2.011518000
H	0.778859000	-3.117511000	0.615089000
H	2.055220000	0.801618000	3.379168000
H	2.754661000	-0.521387000	4.324892000
H	0.532250000	-1.604699000	4.512783000
H	0.316992000	0.066511000	5.027828000
H	2.635496000	0.780466000	0.346157000
H	4.744955000	1.164169000	-0.857910000
H	6.763364000	-0.187752000	-0.300061000
H	6.615219000	-1.947794000	1.448841000
H	4.473614000	-2.365396000	2.604054000
H	-2.660576000	0.754865000	2.009211000
H	-4.963641000	-0.121976000	2.047788000
H	-5.455970000	-2.288343000	3.167818000
H	-3.613393000	-3.539691000	4.268185000
H	-1.324496000	-2.650852000	4.252030000
H	-0.504223000	-2.657123000	-4.536100000
H	-1.302967000	-3.595232000	-3.279047000
H	-3.027311000	-2.106726000	-4.257954000
H	-1.961664000	-0.720635000	-4.045177000
H	2.386352000	-1.154950000	-1.730642000
H	4.247440000	-2.482036000	-0.828186000
H	4.009523000	-4.945846000	-0.557763000
H	1.887659000	-6.047557000	-1.237253000
H	0.040965000	-4.723336000	-2.158170000
H	-4.677783000	-1.564830000	-0.284173000
H	-6.505775000	0.043895000	0.097549000
H	-6.738126000	2.040350000	-1.363589000
H	-5.112966000	2.399326000	-3.208386000
H	-3.291034000	0.805683000	-3.584838000
H	-3.136003000	-2.500725000	-1.853296000
H	0.369286000	-1.047497000	-2.930406000
H	-0.493611000	0.755696000	2.867755000
H	2.129649000	-2.150651000	2.612588000
H	2.157132000	0.987806000	-2.297230000
H	-1.511753000	4.899050000	-0.318823000
H	0.146737000	5.328473000	-0.786467000
H	-0.192959000	6.871600000	1.073100000
H	-1.231152000	5.714455000	1.917469000
H	0.826349000	5.208673000	3.100293000
H	1.813084000	5.629151000	1.698488000
C	-2.555976000	2.423560000	-0.272415000
H	-3.238071000	1.574906000	-0.279631000
H	-2.370386000	2.708067000	0.765346000
H	-3.078374000	3.253138000	-0.761595000
H	-1.314456000	1.871082000	-2.035036000
C	4.035859000	2.508386000	-4.033525000
H	3.782384000	3.468685000	-4.504737000
H	4.936856000	2.122124000	-4.516510000
H	3.215564000	1.805831000	-4.242011000
H	3.463406000	2.959998000	-2.217033000
O	4.296343000	2.641819000	-2.645208000

Pro-(*R*) (C2) with the explicit Solvent-substrate interaction

G298K= -2834.081423
Img. Freq.=-1030.4292

C	3.874177000	1.785128000	0.029198000
C	3.248678000	2.079020000	1.250087000
C	3.055035000	3.424529000	1.580595000
C	3.482460000	4.442666000	0.726448000
C	4.102449000	4.135405000	-0.481526000
C	4.291824000	2.797023000	-0.828674000
C	2.810446000	0.940338000	2.146551000
C	2.383015000	1.300407000	3.581659000
C	1.669843000	0.079290000	4.166065000
C	0.574618000	-0.316508000	3.157838000
C	-0.100553000	-1.647013000	3.369499000
C	-1.486821000	-1.755055000	3.195560000
C	-2.137721000	-2.977892000	3.337843000
C	-1.413767000	-4.124630000	3.660523000
C	-0.036302000	-4.029457000	3.856162000
C	0.611529000	-2.803424000	3.718527000
P	1.348089000	-0.050483000	1.441306000
C	2.148071000	-1.670187000	0.971570000
C	1.147858000	-2.581908000	0.246599000
P	0.237393000	-1.684398000	-1.106898000

Co	-0.043476000	0.466771000	-0.511369000
N	-1.750083000	0.336594000	0.419202000
C	-2.412441000	1.455070000	0.612186000
O	-3.478493000	1.615191000	1.271509000
C	-1.132830000	-2.922903000	-1.535502000
C	-0.922760000	-3.242400000	-3.032599000
C	0.588285000	-3.302794000	-3.280236000
C	1.179980000	-1.999181000	-2.714254000
C	2.676939000	-1.903190000	-2.573533000
C	3.318691000	-0.679690000	-2.812307000
C	4.694591000	-0.544482000	-2.641702000
C	5.460367000	-1.630333000	-2.220049000
C	4.837450000	-2.855804000	-1.988073000
C	3.462247000	-2.991261000	-2.168224000
C	-2.518657000	-2.488993000	-1.130986000
C	-3.143797000	-3.087522000	-0.032104000
C	-4.408823000	-2.675321000	0.387051000
C	-5.072332000	-1.657000000	-0.293050000
C	-4.457054000	-1.052495000	-1.390068000
C	-3.193148000	-1.461402000	-1.802308000
O	-1.224244000	1.046804000	-2.578333000
C	-2.154429000	1.856500000	-2.513894000
N	-2.438934000	2.678743000	-1.478264000
C	-3.707330000	3.396260000	-1.652490000
C	-3.935612000	3.346080000	-3.172044000
C	-3.200898000	2.067371000	-3.597075000
C	-1.795081000	2.638708000	-0.152725000
C	-0.263657000	2.583525000	-0.217633000
H	0.102711000	2.694694000	0.804367000
H	2.583142000	-2.177777000	1.834774000
H	2.970171000	-1.407967000	0.299773000
H	1.637984000	-3.476506000	-0.143213000
H	0.373611000	-2.916135000	0.942686000
H	-1.364761000	-2.457644000	-3.653460000
H	-1.420650000	-4.180356000	-3.291565000
H	1.005627000	-4.175353000	-2.768539000
H	0.826833000	-3.405005000	-4.342416000
H	-2.706084000	-0.946625000	-2.620059000
H	-4.958654000	-0.245543000	-1.912663000
H	-6.053069000	-1.329538000	0.032492000
H	-4.873195000	-3.150932000	1.243694000
H	-2.629939000	-3.873027000	0.511285000
H	2.731131000	0.173916000	-3.130555000
H	5.169568000	0.409226000	-2.840852000
H	6.530463000	-1.525126000	-2.083298000
H	5.422549000	-3.711385000	-1.669804000
H	3.003995000	-3.956192000	-1.990596000
H	1.231269000	0.292355000	5.145324000
H	2.387232000	-0.735153000	4.303284000
H	3.245361000	1.605732000	4.180380000
H	1.682038000	2.140977000	3.571897000
H	-2.058241000	-0.868441000	2.945833000
H	-3.210188000	-3.032464000	3.194068000
H	-1.917509000	-5.078537000	3.766869000
H	0.537353000	-4.911184000	4.119496000
H	1.680856000	-2.754846000	3.882497000
H	4.031502000	0.751385000	-0.257121000
H	4.768495000	2.542496000	-1.768390000
H	4.430774000	4.925947000	-1.146616000
H	3.324395000	5.477695000	1.008647000
H	2.575091000	3.694670000	2.512450000
H	3.638043000	0.225499000	2.210642000
H	-0.200031000	0.455625000	3.183990000
H	0.840132000	-1.174088000	-3.347010000
H	-0.875140000	-3.822068000	-0.968102000
C	0.286775000	3.743920000	-1.060475000
H	-2.212802000	-0.477694000	0.807454000
H	-3.617367000	4.412462000	-1.264205000
H	-4.498813000	2.886035000	-1.093030000
H	-4.994549000	3.344414000	-3.429570000
H	-3.471235000	4.215973000	-3.641682000
H	-2.733004000	2.115419000	-4.580593000
H	-3.858985000	1.191855000	-3.587406000
H	0.028870000	3.627600000	-2.116423000
H	-0.128586000	4.701408000	-0.721032000
H	1.373443000	3.805332000	-0.981456000
H	-2.096371000	3.564938000	0.346437000
H	1.221103000	0.862986000	-1.331333000
H	0.732907000	1.685520000	-0.979563000
C	-1.722172000	3.163587000	3.526264000
H	-1.297945000	3.925336000	4.184910000
H	-2.020043000	2.304160000	4.142907000
H	-0.927609000	2.828372000	2.844848000
H	-3.199021000	3.026896000	2.270750000
O	-2.820131000	3.739230000	2.831943000